Coverage Analysis of Multi-Stream MIMO HetNets With MRC Receivers

Mohammad G. Khoshkholgh, Keivan Navaie, *Senior Member, IEEE*, Kang G. Shin, *Life Fellow, IEEE*, and Victor C. M. Leung, *Fellow, IEEE*

***Abstract*— Most of the current research on the coverage performance of multi-stream MIMO heterogeneous networks (HetNets) has focused on a single data-stream. This does not always provide accurate results as our analysis show the cross-stream correlation due to interference can greatly affect the coverage performance. This paper analyzes the coverage probability in such systems, and studies the impact of cross-stream correlation. Specifically, we focus on the max-SIR cell association policy and leverage stochastic geometry to study scenarios, whereby a receiver is considered in the coverage, if all of its data-streams are successfully decodeable. Assuming open-loop maximum ratio combining (MRC) at receivers, we consider the cases where partial channel state information is available at the receiver. We then obtain an upper-bound on the coverage and formulate cross-stream SIR correlation. We further show that approximating such systems based on fully-correlated (non-correlated) data-streams results in a slight underestimation (substantial overestimation) of the coverage performance. Our results provide insights on the multiplexing regimes where densification improves the coverage performance and spectral efficiency. We also compare MRC with more complex zero-forcing receiver and provide quantitative insights on the design tradeoffs. Our analysis is validated via extensive simulations.**

***Index Terms*— Densification, heterogeneous networks (HetNets), multiple-input multiple-output (MIMO), multiplexing gain, network-wise coverage performance, signal-to-interference ratio (SIR) correlation, stochastic geometry.**

I. Introduction

SPECTRAL efficiency in heterogenous networks (HetNets) is substantially enhanced using densification and universal frequency reuse. A key physical-layer component of dense HetNets is MIMO technology which is also capable of meeting the high demand for wireless bandwidth [2], [3]. Nevertheless, macroscopic (network-level) performance, where MIMO multiplexing communication is utilized in conjunction with densification and heterogeneity, still remains to be explored.

Conventionally, MIMO systems are analyzed for isolated scenarios, where only point-to-point, single cell, and/or clustered communications are considered [4], [5]. Such analyses can characterize the various design aspects of MIMO HetNets, but they cannot capture the macroscopic performance of MIMO systems under severe and heterogenous inter-cell interference (ICI), commonly seen in dense HetNets with aggressive frequency reuse. We would like to address this very issue by using stochastic-geometry-based analytical techniques.

Stochastic geometry has been widely used for modeling and performance evaluation of wireless cellular networks, including HetNets, e.g., [6]–[10]. Using these techniques enables incorporation of impacts of line-of-sight propagation, path-loss models, and blockage effect into the network-wise evaluation of spectral efficiency without compromising the tractability and accuracy of the analysis [8], [10], [11].

A. Related Work

Reviewed below are the related studies of the performance of MIMO systems. This work is related to multi-stream (multiplexing) MIMO in the context of ad hoc communications, see, e.g., [12]–[15]. The results for ad hoc systems, however, are not necessarily valid in the context of cellular networks which is the subject of this paper, due mainly to the fundamental differences between them attributed to their association mechanisms and MAC protocols.

The adopted cell-association (CA) policy plays a crucial role in the performance of MIMO HetNet systems. In a given coverage area, cell association determines which BS to serve a given mobile user. Different CA approaches are categorized as *range expansion* and *Max-SIR association*.

In [16] the coverage probability of interference blind maximum ratio combining (IB-MRC) as well as optimal combining (OC) receiver techniques were analyzed for a system with orthogonal space time transmission at the BSs. The main focus of [17] was on the uplink under power control and OC. Symbol error probability (SEP) of MIMO multiplexing systems was then analyzed in [18], where Gil-Pelaez inversion theorem [11] was used in the derivations. Equivalent-in distribution (EiD) notion was developed further in [19] to quantify SEP, using a single integral formula when noise level was negligible. The authors of [19] covered receive-diversity, multiplexing, and orthogonal space-time systems. Similar to [19], the work of [20] proposed a new technique to model ICI based on a

Manuscript received March 6, 2017; revised July 1, 2017; accepted September 14, 2017. Date of publication September 22, 2017; date of current version December 8, 2017. This work was supported in part by the National Natural Science Foundation of China under Grant 61671088, in part by the Vanier Canada Graduate Scholarship, and in part by the Canadian Natural Sciences and Engineering Research Council. This paper was presented at the IEEE 84th Vehicular Technology Conference, Montreal, Canada, September 2016 [1]. The associate editor coordinating the review of this paper and approving it for publication was T. Lok. *(Corresponding author: Victor C. M. Leung)*

M. G. Khoshkholgh is with the Department of Electrical and Computer Engineering, The University of British Columbia, Vancouver, BC V6T 1Z4, Canada (e-mail: m.g.khoshkholgh@gmail.com).

K. Navaie is with the School of Computing and Communications, Lancaster University, Lancaster LA1 4WA, U.K. (e-mail: k.navaie@lancaster.ac.uk).

K. G. Shin is with the Department of Electrical Engineering and Computer Science, University of Michigan, Ann Arbor, MI 48109-2121 USA (e-mail: kgshin@umich.edu).

V. C. M. Leung is with the Department of Electrical and Computer Engineering, The University of British Columbia, Vancouver, BC V6T 1Z4, Canada, and also with the School of Information and Electronic Engineering, Zhejiang Gongshang University, Hangzhou 310018, China (e-mail: vleung@ieee.org).

Color versions of one or more of the figures in this paper are available online at http://ieeexplore.ieee.org.

Digital Object Identifier 10.1109/TWC.2017.2753771

Gaussian distribution in order to develop a unified framework for the evaluation of coverage probability and data rate of MIMO cellular systems.

In general however, range-expansion CA does not distinguish between the corresponding MIMO techniques in the CA stage. Therefore, in many cases mentioned above, the CA policy is in fact a replica of the one considered in the SISO counterpart [7], [9]. This makes range expansion defiant in effectively incorporating the attributes of MIMO communications to improve multiplexing and diversity. That is one of the reasons why heuristic offloading procedures are often required to optimize the system performance [21]–[23].

Furthermore, the performance expressions provided in the previous studies often require single/double integrations of (double) higher-order (as many as the number of antennas) derivatives of sophisticated functions, e.g., hypergeometric. For systems with multiple tiers and larger arrays, such expressions become even more complex, making their utilization harder in the system design process. In contrast to this previous work, the coverage expressions obtained in this paper are in closed-form, and their corresponding computation complexities are significantly lower.

On the other hand, the coverage is directly related to signal-to-interference (SIR) distribution. In addition, many network management functions, such as handover and fractional frequency reuse, often operate based on the SIR (or a function thereof) as the main decision metric. These justify consideration of CA rules based on the SIR characteristics.

The authors of [6], [24], and [25] considered max-SIR CA in which the serving BS is the one that provides the maximum SIR. For MISO systems, the authors of [26] provided ordering results on the coverage, capacity, and ASE, and compared several beamforming techniques. In [27], we proposed a flexible max-SIR CA rule tailored for MISO space-division multiple access (SDMA) systems. Algorithms for specifying the number of required SIR measurements before choosing the supporting BS in order to optimize the coverage probability/spectral efficiency were also developed in [27].

Unlike the range-expansion technique for which various aspects of coverage performance have been investigated, the coverage performance of multi-stream MIMO-MRC communications with max-SIR CA is yet to be explored. The main objective of this paper is to analyze the coverage performance of MIMO communication with max-SIR CA rule, where multiple streams are transmitted at the same time. Note that in the literature of multi-stream MIMO communications, the coverage probability of the network is often estimated from the perspective of a given data stream. The thus-obtained coverage for a given data stream is then treated as the coverage performance of the multiplexing (multi-stream) system, see, e.g., [12], [14]–[16], [28]. Nevertheless, such approach may cause substantial error in the evaluation of the coverage probability of multi-stream MIMO HetNets, as the possible correlation across data streams are entirely overlooked.

In fact, when the SIR values among data streams are correlated, the *stream-level* performance that considers the reception quality of a single data stream independent from the others, becomes inadequate. This is because the successful decoding of a data stream is partially dependent upon the decoding status of other data streams. Therefore, the coverage performance of MIMO multiplexing systems from a *link-level* perspective that considers the reception of all the data steams becomes crucial. For range expansion CA, most of the work in the literature focused on multi-user MISO-SDMA systems, e.g., [21]–[23], [29]–[34]. Our work is different from this family of work due to the notion of link-level coverage performance. Note that the other issues studied in this paper — i.e, evaluation of the cross-stream SIR correlation and understanding its impacts on the coverage probability — are irrelevant to MISO-SDMA systems. We previously studied the coverage probability of MIMO multiplexing systems from a link-level perspective [1], [35], [36]. The focus of [35] was on multi-stream MIMO systems where the pre-coding and decoding filters at the transmitter and receiver was constructed according the singular value decomposition (SVD) technique. This techniques however requires perfect and timely CSI at both the transmitter and receiver, which imposes high signaling overhead particularly in dense configurations. Furthermore, in [36], we investigated the link-level coverage performance for multi-stream MIMO networks with zero-forcing beamforming (ZFBF) receivers. The simulation results in [36] show subtle differences between link-level, and stream-level coverage performance in a multi-stream MIMO system. Despite its importance, to the best of our knowledge, the roots and scales of such a discrepancy has not yet been investigated in the related literature.

On the other hand, in SIMO ad hoc networks, the ICI is shown to result in a high correlation among impinged signals across different receive antennas, see, e.g., [37], [38]. Such a correlation compromise the otherwise achievable diversity gain in cases where signals across antennas are independent. This is because in the presence of ICI, the path-loss fluctuations invoke (statistically) correlated interference among antennas due to the common locations of interferers. A similar conclusion was drawn in [16], where the interference correlation was investigated in space-time MIMO ad hoc networks. It was also shown in [16] that ignoring interference correlation among antennas may, in some cases, substantially compromise the accuracy of the analysis. The analysis in [16] is, however, limited to the CDF distribution of an individual data stream, thus being unable to depict the impact of correlation on the CDF distribution of a communication link with a set of data streams.

B. Contributions and Organization

In this paper, we investigate cross-stream SIR correlation and its impacts on the link-level coverage probability in MIMO multiplexing systems. We mainly focus on the maximum ratio combining (MRC) receivers. Note that compared to the ZFBF, the coverage evaluation of the MRC is more challenging due to the cross-stream interference. The coverage performance of MIMO-MRC systems from the *stream-level perspective* is studied in the context of ad hoc communications, e.g., [15]. The results in an ad hoc context are not necessarily extendable to cellular networks because, unlike cellular systems, ad hoc communications often operate without a CA mechanism and lack a central scheduler.

Here we evaluate the MIMO-MRC coverage probability from a link-level perspective in cellular networks. Despite the popularity and practical significance of an MIMO-MRC system for cellular communications due to its simple implementation and near zero feedback overheads, its performance in HetNet settings has not yet been investigated. Our model and analysis are concerned with scenarios that channel state information (CSI) is not available at the BSs and only partially known at the UEs. This paper makes the following two main contributions.

- We obtain a closed-form and easy-to-compute tight upper bound on the network coverage probability for cases where successful decoding of all transmitted data streams is required. The unique feature of our analysis is to accurately incorporate SIR correlation. Our analytical results—supported by extensive simulations—provide significant practical insights on the impacts of densification on the link-level coverage performance. Based on this result, we conclude that improvement in the network coverage performance and area spectral efficiency (ASE) by densification is subject to careful selection of multiplexing gains in different tiers.
- Our analysis also provides insights on important design issues. We present cases where the analysis can be exploited to obtain the coverage performance of pertinent MIMO systems, including ZFBF, when CSI is accurate. Although ZFBF generally outperforms MRC in terms of coverage probability, we demonstrate practical cases in which the high processing costs of ZFBF justifies using MRC. We further provide quantitative insights on the coverage cost of adopting MRC compared to ZFBF and also techniques to control the shrinkage of coverage footprint. We also quantify the trade-off between densification and multiplexing gains in multi-stream MRC systems. Our results indicate that increasing CSI inaccuracy compromises the coverage advantage of multi-stream over single-stream systems.
- We also analyze the cross-stream SIR correlation amongst multiple streams in a communication link. Our analysis provides quantitative insights on the impact of tiers' BSs density, path-loss exponent, CSI inaccuracy, and multiplexing gains on the SIR correlation among data streams. To understand the impacts of SIR correlation on the coverage probability, we then obtain the closed-form bounds on the coverage probabilities for two extreme settings: full SIR correlation (FC) among data streams, and no SIR correlation (NC) among data streams. We then show that the NC setting substantially over-estimates the coverage performance while the FC setting slightly underestimates it.

Finally, compared to [1], our analysis includes CSI inaccuracy, and the coverage probability is now expressed in a closed-form. We also study the effect of cross-stream SIR correlation on the coverage probability and provide various engineering insights and system designs.

The rest of the paper is organized as follows. Section II presents the system model and Section III provides coverage evaluation. Section IV investigates the SIR correlation and its impact on the coverage probability. The simulation results are provided in Section V followed by conclusions in Section VI.

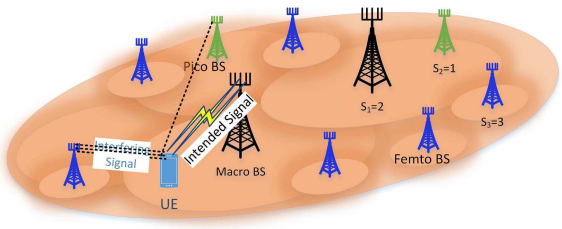

Fig. 1. A schematic of the considered system model. For simplicity only a small sample of the network is depicted.

II. System Model

We consider the downlink in a heterogeneous cellular network (HetNet) consisting of $K \geq 1$ tiers of randomly located base-stations (BSs). In each tier $i \in \mathcal{K}$, BSs are spatially distributed according to a homogenous Poisson Point Process (PPP), Φ_i, with a given spatial density, $\lambda_i \geq 1$ [6]. For mathematical tractability, we assume that the PPPs corresponding to each tier are mutually independent. Therefore, each tier i can be completely characterized by the spatial density of its BSs, λ_i, their transmit power, P_i Watts, the corresponding SIR threshold at the receivers, $\beta_i \geq 1$, the number of BS's transmit antennas N_i^t, and the number of scheduled streams $S_i \leq \min\{N_i^t, N^r\}$ (also referred to as the *multiplexing gain*), where N^r is the number of antennas at the user equipments (UEs) (see Fig. 1).

In the model under consideration, S_i data streams are considered in each tier/BS as parallel flows of information as in [12] and [15]. UEs are randomly located across the network coverage area and form a PPP, Φ_U, with density $\lambda_U \gg \sum_i \lambda_i$, independent of $\{\Phi_i\}$s. Similar to [16], [26], and [39], we further assume that in each active cell, only one UE is served at each time slot. If more than one UE are associated with a given BS, we adopt time-sharing per cell for scheduling the UEs.

Considering the stationarity of the point processes, according to Slivnayak's theorem, we can investigate spatial network performance from the perspective of a UE located at the origin [40], [41]; we will refer to such an UE the *typical UE*.

Let $\boldsymbol{H}_{x_i} \in \mathbb{C}^{N^r \times S_i}$ be the fading channel matrix between BS x_i and the typical UE, where each entry is independently drawn from a complex Gaussian random variable with zero mean and unit variance, $\mathcal{CN}(0, 1)$, i.e., Rayleigh fading assumption.

Here we focus on the scenarios that only partial CSI is available at the receivers. As in [42] and [43], the quantified measure for channel estimation error is considered to be the correlation coefficient between the actual fading channel coefficient and its estimated value as $\boldsymbol{H}_{x_i} = \sqrt{1-\epsilon_i^2}\ \widetilde{\boldsymbol{H}}_{x_i} + \epsilon_i \boldsymbol{E}_{x_i}$, where $\widetilde{\boldsymbol{H}}_{x_i}$ is the estimated channel which is a complex Gaussian random matrix with zero mean and identity covariance matrix; ϵ_i^2 measures the inaccuracy of channel estimation;

and $\boldsymbol{E}_{x_i}$ is a complex Gaussian random matrix with zero mean and identity covariance matrix. Random variables $\boldsymbol{E}_{x_i}$ and $\widetilde{\boldsymbol{H}}_{x_i}$ are assumed independent, e.g., in cases where CSI is estimated using a pilot-based minimum mean square error (MMSE) [42], [43].

For the typical UE associated with BS x_i transmitting S_i data streams, the received signal, $\boldsymbol{y}_{x_i} \in \mathbb{C}^{N^r \times 1}$, is:

$$\boldsymbol{y}_{x_i} = \|x_i\|^{-\frac{\alpha}{2}}\sqrt{1-\epsilon_i^2}\widetilde{\boldsymbol{H}}_{x_i}\boldsymbol{s}_{x_i} + \|x_i\|^{-\frac{\alpha}{2}}\epsilon_i \boldsymbol{E}_{x_i}\boldsymbol{s}_{x_i} + \sum_{j\in\mathcal{K}}\sum_{x_j\in\Phi_j/x_0} \|x_i\|^{-\frac{\alpha}{2}}\boldsymbol{H}_{x_j}\boldsymbol{s}_{x_j}, \quad (1)$$

where $\boldsymbol{s}_{x_i} = [s_{x_i,1}\ldots s_{x_i,S_i}]^T \in \mathbb{C}^{S_i\times 1}$, so that $s_{x_i,l} \sim \mathcal{CN}(0, P_i/S_i)$, is the transmitted streams at BS x_i; $\|x_i\|^{-\alpha}$ is the distance-dependent path-loss attenuation; $\|x_i\|$ denotes the Euclidian distance between BS x_i and the origin; and $\alpha > 2$ is the path-loss exponent. We further assume that the transmitted signals as well as channel matrices are independent. The first term in (1) accounts for the useful signal, the second term represents the interference due to inaccuracy of CSI, and the last term is the ICI. At the receiver, maximum ratio combining (MRC) [15] is adopted with decoding filter $\boldsymbol{U}_{x_i} = \boldsymbol{H}_{x_i} = [\boldsymbol{h}_{x_i,1}\ldots\boldsymbol{h}_{x_i,S_i}]$. Post-processing SIR for data stream l_i is therefore given by Eq. (6) on bottom of the 6th page.

We then set random variable (r.v.) $H^{\mathrm{MRC}}_{x_i,l_i} \triangleq \|\tilde{\boldsymbol{h}}_{x_i,l_i}\|^2$ which is chi-squared with $2N^r$ degrees-of-freedom (DoFs). Further, we define r.v.s $\hat{H}^{\mathrm{MRC}}_{x_i,l_i} \triangleq \sum_{l'\neq l_i} \frac{\|\tilde{\boldsymbol{h}}^{\dagger}_{x_i,l_i}\boldsymbol{h}_{x_i,l'}\|^2}{\|\tilde{\boldsymbol{h}}_{x_i,l_i}\|^2}$ which is also chi-squared with $2(S_i-1)$ DoFs, and $\tilde{H}^{\mathrm{MRC}}_{x_i,l_i} \triangleq \frac{\|\tilde{\boldsymbol{h}}^{\dagger}_{x_i,l_i}\boldsymbol{e}_{x_i,l_i}\|^2}{\|\tilde{\boldsymbol{h}}_{x_i,l_i}\|^2}$ which is an exponential r.v. Both $\hat{H}^{\mathrm{MRC}}_{x_i,l_i}$ and $\tilde{H}^{\mathrm{MRC}}_{x_i,l_i}$ are independent of $H^{\mathrm{MRC}}_{x_i,l_i}$. We further set $G^{\mathrm{MRC}}_{x_j,l_i} \triangleq \sum_{l_j=1}^{S_j} \frac{\|\tilde{\boldsymbol{h}}^{\dagger}_{x_i,l_i}\boldsymbol{h}_{x_j,l_j}\|^2}{\|\tilde{\boldsymbol{h}}_{x_i,l_i}\|^2}$ which is also chi-squared with $2S_j$ DoFs and independent of $\hat{H}^{\mathrm{MRC}}_{x_i,l_i}$, $\tilde{H}^{\mathrm{MRC}}_{x_i,l_i}$, and $H^{\mathrm{MRC}}_{x_i,l_i}$. Using the above notation, $H^{\mathrm{MRC}}_{x_i,l_i}$, $\hat{H}^{\mathrm{MRC}}_{x_i,l_i}$, $\tilde{H}^{\mathrm{MRC}}_{x_i,l_i}$, and $G^{\mathrm{MRC}}_{x_j,l_i}$, respectively, stand for the channel power gains associated with the intending the l_i-th data stream, the interference on stream l_i due to imperfect CSI estimation, the inter-stream interference caused by streams $l_i' \neq l_i$, and the ICI imposed by $x_j \neq x_i$. Post-processing SIR in (6) is then represented as

$$\mathrm{SIR}^{\mathrm{MRC}}_{x_i,l_i} = \frac{\frac{P_i}{S_i}\|x_i\|^{-\alpha}(1-\epsilon_i^2)H^{\mathrm{MRC}}_{x_i,l_i}}{\frac{P_i}{S_i\|x_i\|^{\alpha}}\left(\hat{H}^{\mathrm{MRC}}_{x_i,l_i} + \epsilon_i^2\tilde{H}^{\mathrm{MRC}}_{x_i,l_i}\right) + \sum_{j\in\mathcal{K}}\sum_{x_j\in\Phi_j/x_i}\frac{P_j G^{\mathrm{MRC}}_{x_j,l_i}}{S_j\|x_j\|^{\alpha}}}. \quad (2)$$

Eq. (2) incorporates per-stream transmission power, multiplexing gains, ICI, CSI inaccuracy, and inter-stream interference.

III. Coverage Performance Evaluation

A. Coverage Performance in Multi-Stream MIMO Systems

In HetNets, similar to other wireless networks, the SIR is translated into practical performance metrics, such as the coverage probability. For a given coverage probability, one can then, among other parameters, evaluate the required density of the BSs in each tier and/or their multiplexing gains. In the case of a HetNet with single-stream transmission, the coverage probability in a tier, i, is directly related to the cumulative distribution function (CDF) of the corresponding SIR. More specifically, for tier i, the coverage probability is often defined as the probability that the SIR stays above a given threshold, β_i, throughout the coverage area. In the case of multiple streams however, depending on the transceiver structure and/or the quality requirements, evaluating the coverage probability becomes more complex.

In some transceiver techniques, the coverage probability depends upon the CDF of the weakest SIR value among S_i streams [44]–[47]. Thus, a UE is considered in the coverage if all of its streams are successfully decoded; this is referred to *all-coverage probability*, as in the isolated scenarios [47], [48].[1]

To specify the CA policy, we focus on the max-SIR CA rule as in [6], [26], and [36], where a typical UE is associated with a BS that provides the strongest SIR. To evaluate the all-coverage probability, we adopt the max-SIR CA rule of [36] which is an extension of the one considered in [6], [26], and [27], to the multi-stream MIMO communications: the associated BS is the one whose corresponding minimum SIR value (measured across streams) is the maximum among all the BSs. For brevity, we will henceforth refer to the all-coverage probability as the coverage performance. A typical UE is thus in the coverage if the set

$$\mathcal{A}^{\mathrm{MRC}}_{\mathrm{all}} = \left\{\exists i \in \mathcal{K} : \max_{x_i\in\Phi_i}\min_{l_i=1,\ldots,S_i}\mathrm{SIR}^{\mathrm{MRC}}_{x_i,l_i} \geq \beta_i\right\}, \quad (3)$$

is nonempty and the coverage probability is defined as $\mathcal{P}^{\mathrm{MRC}}_C = \mathbb{P}\{\mathcal{A}^{\mathrm{MRC}}_{\mathrm{all}} \neq \emptyset\}$.

B. The Coverage Probability

Analytical evaluation of $\mathcal{P}^{\mathrm{MRC}}_C$ is rather complex due mainly to the cross stream SIR correlation, non-Rayleigh-type fluctuations, CSI inaccuracy, and also the inter-stream interference. In the following proposition, we provide an analytical upper bound on the coverage probability.

Proposition 1: In a MIMO-MRC system adopting the maximum SIR CA rule, the coverage probability is upper-bounded as:

$$\mathcal{P}^{\mathrm{MRC}}_C \leq \frac{\pi}{\tilde{C}(\alpha)}\sum_{i\in\mathcal{K}}\frac{\lambda_i\left(\frac{P_i(1-\epsilon_i^2)}{S_i^2\beta_i}\right)^{\breve{\alpha}}(\Theta(\beta_i,\epsilon_i,S_i))^{S_i}}{\sum_{j=1}^{K}\lambda_j\left(\frac{P_j}{S_j}\right)^{\breve{\alpha}}\left(\frac{\Gamma(\frac{\breve{\alpha}}{S_i}+S_j)}{\Gamma(S_j)}\right)^{S_i}}, \quad (4)$$

where letting $\mathrm{B}(a,b) = \frac{\Gamma(a)\Gamma(b)}{\Gamma(a+b)}$ be the beta function, $\Theta(\beta_i,\epsilon_i,S_i)$ is given by Eq. (7) on bottom.

Proof: See Appendix-A.

[1] Note that if the original data streams are spatially coded across multiple data streams, then *sum-coverage probability* is a relevant metric, whereby the accumulated transmitted data rate must be large enough for a link to be considered in coverage [13], [47]. We exclude such cases and focus on the all-coverage probability.

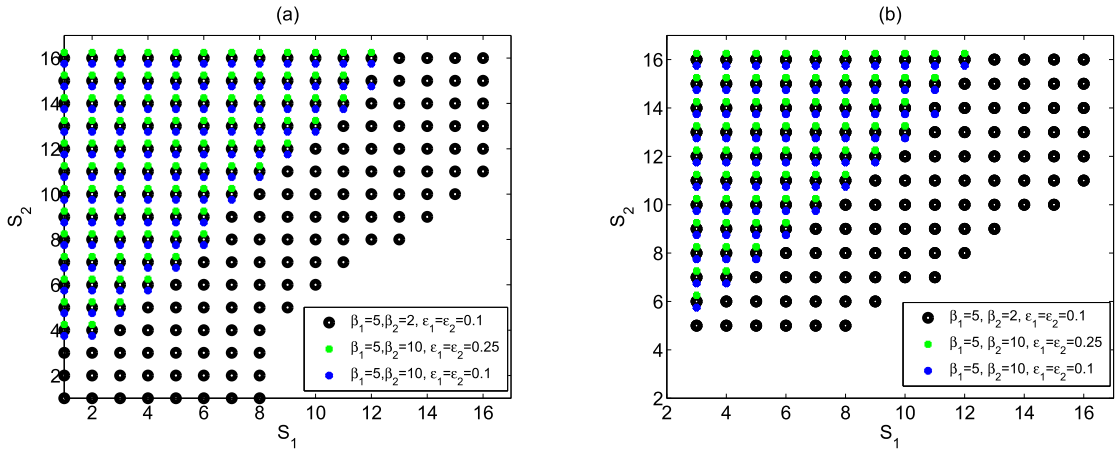

Fig. 2. (a) Combinations of multiplexing gains for which $\frac{\partial \mathcal{P}_C^{\mathrm{MRC}}}{\partial \tilde{\lambda}_1} > 0$; (b) Combinations of multiplexing gains for which $\frac{\partial \mathrm{ASE}_{\mathrm{all}}^{\mathrm{MRC}}}{\partial \tilde{\lambda}_1} > 0$. Parameters are $\alpha = 4$, $P_1 = 50$W, and $P_2 = 1$W.

Despite significant model complexities, Proposition 1 provides a closed-form upper-bound for the coverage probability. It is difficult to quantify the accuracy of the derived upper-bound as G_{j,l_i}^{MRC}s are random in nature and t_{l_i}s are integral variables. However, our simulation results in Section V indicate that the upper-bound of Proposition 1 is accurate and representative.

The bound on the coverage probability in (4) shows the effects of many important parameters such as the BS deployment density in each tier, their TX power and multiplexing gain, CSI inaccuracies, and the corresponding tiers' SIR threshold. The impact of the number of receive antennas is captured via parameter $\Theta(\beta_i, \epsilon_i, S_i)$ in (7). Note that the numerator and denominator of (4) correspond to the intended communication link, and the ICI, respectively.

A close examination of (4) in Proposition 1 provides significant insights on important design aspects of HetNets which are discussed in the following subsections.

C. Is Densification Always Beneficial?

1) Does Densification Always Improve the Coverage Probability?: We investigate the impact of densification on the coverage probability. We are interested in combinations of system parameters for which the coverage probability is increased by increasing the density of the BS in a given tier, namely tier 1: $\frac{\partial \mathcal{P}_C^{\mathrm{MRC}}}{\partial \tilde{\lambda}_1} > 0$. For brevity, we set $K = 2$, and $\tilde{\lambda}_1 = \lambda_1 (P_1/S_1)^{\breve{\alpha}}$, $\tilde{\lambda}_2 = \lambda_2 (P_2/S_2)^{\breve{\alpha}}$, $A_{ji} = \left(\frac{\Gamma(\frac{\breve{\alpha}}{S_i}+S_j)}{\Gamma(S_j)}\right)^{S_i}$. In this case, it can be shown that for $\frac{\partial \mathcal{P}_C^{\mathrm{MRC}}}{\partial \tilde{\lambda}_1} > 0$, it is necessary to have $\frac{\tilde{\lambda}_2}{\tilde{\lambda}_1}(A_{21} - BA_{22}) < A_{12}B - A_{11}$, where $B = \sqrt{\left(\frac{(1-\epsilon_1^2)\beta_2 S_2}{(1-\epsilon_2^2)\beta_1 S_1}\right)^{\breve{\alpha}} \frac{(\Theta(\beta_1,\epsilon_1,S_1))^{S_1} A_{21}}{(\Theta(\beta_2,\epsilon_2,S_2))^{S_2} A_{12}}}$. Fig. 2.a shows various combinations of the multiplexing gains that guarantee $\frac{\tilde{\lambda}_2}{\tilde{\lambda}_1}(A_{21} - BA_{22}) < A_{12}B - A_{11}$. In general, for densification of tier 1 to be effective in improving coverage performance, we need $S_2 > S_1$. In fact, as decoding S_2 data streams is more unlikely than S_1 data streams, densification of tier 1 allows UEs to be more frequently be associated with tier 1, thus improving the coverage probability. Moreover, by increasing β_1 or CSI inaccuracy, we get a smaller number of multiplexing gain combinations, (S_1, S_2), in which densification improves the coverage probability.

2) Does Densification Always Improve the Area Spectral Efficiency (ASE)?: Area Spectral Efficiency (ASE) is an essential performance metric which indicates efficiency of spectral usage throughout the coverage area of a wireless network. In a MIMO HetNet, the data rate of tier i is $S_i \log(1+\beta_i)$, therefore, $\mathrm{ASE}^{\mathrm{MRC}} = \sum_i \lambda_i S_i \mathcal{P}_{C,i}^{\mathrm{MRC}} \log(1+\beta_i)$, where $\mathcal{P}_{C,i}^{\mathrm{MRC}}$ denotes the probability that a BS in tier i is being successfully associated with the typical UE. Using Proposition 1, we then write $\mathcal{P}_{C,i}^{\mathrm{MRC}} \leq \frac{\pi}{\tilde{C}(\alpha)} \frac{\lambda_i \left(\frac{P_i}{S_i^2 \beta_i}\right)^{\breve{\alpha}} (\Theta(\beta_i,\epsilon_i,S_i))^{S_i}}{\sum_{j=1}^{K} \lambda_j \left(\frac{P_j}{S_j}\right)^{\breve{\alpha}} \left(\frac{\Gamma(\frac{\breve{\alpha}}{S_i}+S_j)}{\Gamma(S_j)}\right)^{S_i}}$. Here we are interested in system parameters combinations so that $\frac{\partial \mathrm{ASE}^{\mathrm{MRC}}}{\partial \tilde{\lambda}_1} > 0$, i.e., densification in tier i, increases the ASE. Straightforward mathematical derivations lead to $\tilde{B}\frac{\frac{\tilde{\lambda}_1}{\tilde{\lambda}_2}A_{12}+A_{22}}{A_{12}} \geq \frac{\frac{\tilde{\lambda}_1}{\tilde{\lambda}_2}A_{11}+A_{21}}{\frac{\tilde{\lambda}_1}{\tilde{\lambda}_2}A_{12}+2A_{21}}$, where $\tilde{B} \triangleq \sqrt{\left(\frac{(1-\epsilon_1^2)\beta_2 P_2}{(1-\epsilon_2^2)\beta_1 P_1}\right)^{\breve{\alpha}} \frac{(\Theta(\beta_1,\epsilon_1,S_1))^{S_1}\log(1+\beta_1)}{(\Theta(\beta_2,\epsilon_2,S_2))^{S_2}\log(1+\beta_2)}}$. Fig. 2.b shows the combinations of multiplexing gains in which the densification of tier 1 results in an ASE improvement. For $S_2 \geq S_1$, even for small β_1, it is still possible to have a higher multiplexing gain, S_1, while densifying tier 1. Comparison of Figs. 2.a and 2.b further suggests that to improve ASE by densification in tier 1, i.e., increasing λ_1, one needs to have a higher multiplexing gain in tier 2, $S_2 > S_1$.

D. Coverage Performance of Relevant MIMO Communications Scenarios

Although Proposition 1 considers an open-loop tranceiver, one can utilize Proposition 1 to evaluate the coverage probability for various closed-loop scenarios, such as SISO ($N_i^t = N^r = 1, \forall i$) [6], MISO-SDMA ($N^r = 1$) [26], [29], Limited-feedback MISO-SDMA [26], and SIMO ($S_i = 1, \forall i$). This is simply because the corresponding post-processing SIRs in the aforementioned closed loop techniques are often a function of the obtained SIR in (2).

Assuming perfect CSI, immediate extensions of Proposition 1 are for zero-forcing beamforming (ZFBF) at the receiver, and orthogonal space-time block codes (OSTBC). Such extensions can be done after making proper adjustments to the number of DoFs in the desired and interfering signals through the general framework proposed in [15].

E. Selecting the Transceiver Technique

We compare two prevalent open-loop techniques: ZFBF and MRC. Here we assume a perfect CSIR, i.e., $\epsilon_i = 0\ \forall i$. We then set $\Theta^{\mathrm{ZF}}(S_i) \triangleq \sum_{m_i=0}^{N^r-S_i} \frac{\Gamma(\frac{\breve{\alpha}}{S_i}+m_i)}{\Gamma(\frac{\breve{\alpha}}{S_i})\Gamma(1+m_i)}$. The coverage probability of the system with ZFBF was derived in [36] as:

$$\mathcal{P}_C^{\mathrm{ZF}} \leq \frac{\pi}{\tilde{C}(\alpha)} \sum_{i\in\mathcal{K}} \frac{\lambda_i \left(\frac{P_i}{S_i^2\beta_i}\right)^{\breve{\alpha}} (\Theta^{\mathrm{ZF}}(S_i))^{S_i}}{\sum_{j\in\mathcal{K}} \lambda_j \left(\frac{P_j}{S_j}\right)^{\breve{\alpha}} \left(\frac{\Gamma(\frac{\breve{\alpha}}{S_i}+S_j)}{\Gamma(S_j)}\right)^{S_i}}. \quad (5)$$

This is consistent with Proposition 1, as $\mathcal{P}_C^{\mathrm{ZF}}$ in (5) can also be obtained using the bound on $\mathcal{P}_C^{\mathrm{MRC}}$ in Proposition 1, simply by substituting $\Theta(\beta_i, 0, S_i)$ in (4) with $\Theta^{\mathrm{ZF}}(S_i)$.

Using (5) and Proposition 1, we can now inspect whether ZFBF outperforms MRC. For clarity, we set $K = 1$. It is then straightforward to confirm that $\mathcal{P}_C^{\mathrm{ZF}} > \mathcal{P}_C^{\mathrm{MRC}}$ if $\Theta^{\mathrm{ZF}}(S_i) > \Theta(\beta_i, 0, S_i)$. Fig. 3 shows that, in general, ZFBF yields a higher coverage probability than MRC. This is mainly because the MRC receivers suffer from inter-stream interference. Furthermore, as shown in Fig. 3.a, by increasing the multiplexing gain, ZFBF becomes even more efficient than MRC. For a larger N^r, the superiority of ZFBF over MRC is shown to be reduced because the MRC receivers can harness diversity more effectively than ZFBF. Noticing that the ZFBF receiver complexity of a large arrays can be very high (because of the required matrix inversion operation), MRC provides room for compromising coverage performance (in fact, slightly for larger arrays) over computational complexity. Such aspects can be exploited in the design of HetNets. For instance, it is plausible to adaptively select either ZFBF or MRC in order to keep the prescribed coverage performance intact, while minimizing the complexity and energy consumption of the signal processing modules at the receivers.

Fig. 3.b also indicates that for a larger SIR threshold, β, ZFBF significantly outperforms MRC, while for small to moderate values of β, ZFBF is only slightly better than MRC. This observation suggests that for low-rate scenarios (e.g., for the cell-edge UEs) one can trade off a slightly higher performance for a significantly lower computational complexity. Fig. 3 further indicates that the relative performance of ZFBF and MRC is not related to the path-loss exponent.

Spectral efficiency is as important as coverage probability. In what follows, we investigate the impact of using MRC instead on ZFBF on spectral efficiency. Given the simplicity of MRC receivers, we are interested in seeing whether there are cases in which considering both spectral efficiency and the associated computational complexity, it is justifiable to use MRC over ZFBF. We consider the following optimization problem:

$$\begin{aligned} \mathcal{O}_1:\ \eta^*(\zeta_1,\zeta_2) &= \max_{\mathcal{P}_C^{\mathrm{ZF}}-\mathcal{P}_C^{\mathrm{MRC}}\leq\zeta_1} \frac{\sum_i \lambda_i S_i \mathcal{P}_{i,C}^{\mathrm{MRC}} \log(1+\beta_i)}{\sum_i \lambda_i S_i \mathcal{P}_{i,C}^{\mathrm{ZF}} \log(1+\beta_i)} \\ &\quad \times \left(\sum_i \chi_{\frac{\mathrm{ZF}}{\mathrm{MRC}}}(N^r, S_i)\right)^{\zeta_2} \\ &\quad s.t.\ \lambda_i \geq 0, \quad \beta_i \geq 1,\ 1 \leq S_i \leq \min\{N^r, N_i^t\}, \quad \forall i. \end{aligned}$$

In $\mathcal{O}_1$, $\chi_{\frac{\mathrm{ZF}}{\mathrm{MRC}}}(N^r, S_i)$ represents the computational cost compared to MRC (number of arithmetic operations) that is implied by ZFBF in tier i. This parameter incorporates the corresponding computational cost of the required extra matrix multiplication and inversion while using ZFBF. The computational cost, $\chi_{\frac{\mathrm{ZF}}{\mathrm{MRC}}}(N^r, S_i)$, in tier i is formulated as $\chi_{\frac{\mathrm{ZF}}{\mathrm{MRC}}}(N^r, S_i) \propto \mathcal{O}(S_i^2 N^r) + \mathcal{O}((S_i)^{2+c_{\mathrm{inv}}})$ [49]—The first (second) term is associated with the computational cost of matrix multiplication (matrix inversion). For optimized CW-like algorithm's matrix inversion, we have $c_{inv} = 0.373$ [49]. In $\mathcal{O}_1$, $\zeta_2 \geq 0$ represents the level of importance of the computational cost as part of the performance objective. A larger ζ_2 indicates a more importance of the computational cost in the system design, due to battery life, energy consumption, processing power, etc.

In $\mathcal{O}_1$, $\sum_i \lambda_i S_i \mathcal{P}_{i,C}^{\mathrm{ZF}} \log(1+\beta_i)$ further represents the area spectral efficiency (ASE) of MRC and ZFBF techniques, respectively. Note that as in tier i, the number of transmitted data streams is S_i, and thus ASE is proportionally increased by increasing S_i. However, since the coverage probability in each tier is also proportionally reduced by increasing S_i, the growth of S_i may not necessarily result in a higher ASE. The objective of $\mathcal{O}_1$ is to maximize a performance objective including the relative ASE of MRC over ZFBF and the associated computational cost of using ZFBF. This optimization is subject to the required coverage constraint of MRC system

$$\mathrm{SIR}_{x_i,l_i}^{\mathrm{MRC}} = \frac{\frac{P_i}{S_i}\|x_i\|^{-\alpha}(1-\epsilon_i^2)\|\tilde{\boldsymbol{h}}_{x_i,l_i}\|^2}{\frac{P_i}{S_i\|x_i\|^{\alpha}}\left(\sum_{l'\neq l_i}\frac{\|\tilde{\boldsymbol{h}}_{x_i,l_i}^{\dagger}\boldsymbol{h}_{x_i,l'}\|^2}{\|\tilde{\boldsymbol{h}}_{x_i,l_i}\|^2}+\epsilon_i^2\frac{\|\tilde{\boldsymbol{h}}_{x_i,l_i}^{\dagger}\boldsymbol{e}_{x_i,l_i}\|^2}{\|\tilde{\boldsymbol{h}}_{x_i,l_i}\|^2}\right)+\sum_{j\in\mathcal{K}}\sum_{x_j\in\Phi_j/x_i}\frac{P_j}{S_j\|x_j\|^{\alpha}}\sum_{l_j=1}^{S_j}\frac{\|\tilde{\boldsymbol{h}}_{x_i,l_i}^{\dagger}\boldsymbol{h}_{x_j,l_j}\|^2}{\|\tilde{\boldsymbol{h}}_{x_i,l_i}\|^2}}. \quad (6)$$

$$\Theta(\beta_i,\epsilon_i,S_i) \triangleq \sum_{r_i=0}^{N^r-1}\sum_{q_i=0}^{r_i}\sum_{p_i=0}^{q_i}\frac{(-1)^{q_i-p_i}\beta_i^{2q_i-p_i}}{\epsilon_i^{-4q_i+2p_i}(1-\epsilon_i^2)^{S_i}}\frac{\left(1-\epsilon_i^2+\beta_i\right)^{-q_i-S_i+1}\left(1+\epsilon_i^2(\beta_i-1)\right)^{-q_i+p_i-1}}{p_i\mathrm{B}(S_i-1,p_i)(r_i-q_i)\mathrm{B}(\frac{\breve{\alpha}}{S_i},r_i-q_i)}, \quad (7)$$

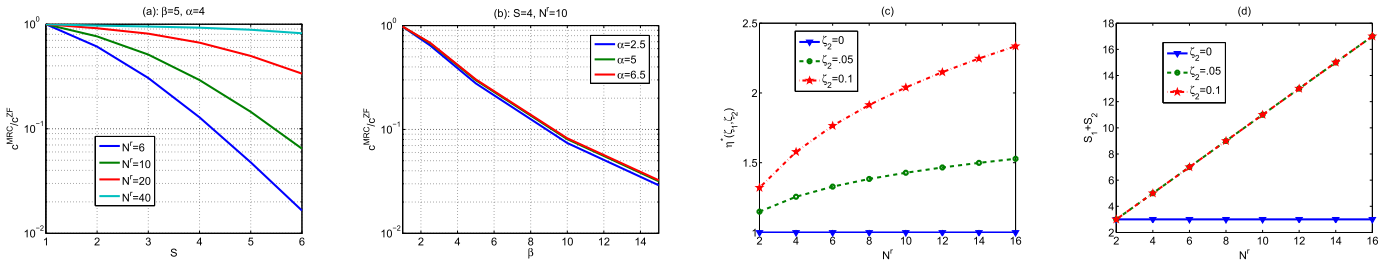

Fig. 3. (a): $\frac{\mathcal{P}_C^{\text{MRC}}}{\mathcal{P}_C^{\text{ZF}}}$, *vs.* the multiplexing gain S; (b): $\frac{\mathcal{P}_C^{\text{MRC}}}{\mathcal{P}_C^{\text{ZF}}}$ *vs.* the SIR threshold β; (c): $\eta^*(\zeta_1, \zeta_2 0)$ *vs.* N^r; (d): $S_1 + S_2$ *vs.* N^r. Parameters are: $\alpha = 4$, $K = 2$, $P_1 = 50$ W, $P_2 = 10$ W.

over ZFBF, i.e., $\mathcal{P}_C^{\text{ZF}} - \mathcal{P}_C^{\text{MRC}} \leq \zeta_1$, where $\zeta_1 \in (0, 1)$ is the maximum acceptable coverage loss compared to ZFBF due to the adoption of MRC. Optimization variables in $\mathcal{O}_1$ are SIR thresholds, deployment densities, and multiplexing gains.

In Fig. 3.c and Fig. 3.d, where we respectively present $\eta^*(\zeta_1 = 0.05, \zeta_2)$, and the total transmitted data streams across tiers, $S_1 + S_2$, versus N^r. In Fig. 3.c, for $\zeta_2 = 0$ (computational cost is not of importance to the system designer) MRC does not show any advantage over ZFBF as both systems have the same ASE. For $\zeta_2 > 0$, however, Fig. 3.c shows that MRC makes a significant performance gain over ZFBF, where the performance measure $\eta^*(\zeta_1 = 0.05, \zeta_2 > 0)$ grows by increasing N^r as well as ζ_2. Fig. 3.d further indicates that $S_1 + S_2$ (multiplexing gain) is increased by increasing N^r. However, by increasing ζ_2 from 0.05 to 0.1, an increase of $\eta^*(\zeta_1 = 0.05, \zeta_2 > 0)$ does not increase the multiplexing gain, $S_1 + S_2$ (see Fig. 3.c), which is due to coverage constraint. The above results suggest that when the computational cost is incorporated, as is the case in practice, MRC appears to be a better option.

IV. Cross-Stream SIR Correlation

As it is also shown in (17), for a given MIMO receiver, the SIR values across streams are statistically correlated mainly because of the correlated interference among antennas due to the common locations of interferers. More specifically, the interference originated from near-by BSs may cause a high level of interference simultaneously to all of the data streams transmitted to a typical UE. As shown in the proof of Proposition 1, the cross-stream SIR correlation renders analytical complexities. In this section, we characterize the aforementioned correlation and analyze its impact on the system coverage performance.

A. SIR Correlation Coefficient

In a link, the coverage probability is related to the joint SIRs' CDF of the streams. Here we focus on the SIR correlation instead of the ICI correlation. To quantify the SIR correlation, the Pearson correlation coefficients is used:

$$\rho_{x_i}^{\text{MRC}}(l_i, l_i') = \frac{\mathbb{E}\left[\text{SIR}_{x_i,l_i}^{\text{MRC}}\text{SIR}_{x_i,l_i'}^{\text{MRC}}\right] - \overline{\text{SIR}}_{x_i,l_i}^{\text{MRC}}\overline{\text{SIR}}_{x_i,l_i'}^{\text{MRC}}}{\sqrt{\text{Var}\left(\text{SIR}_{x_i,l_i}^{\text{MRC}}\right)\text{Var}\left(\text{SIR}_{x_i,l_i'}^{\text{MRC}}\right)}} = \frac{\mathbb{E}\left[\text{SIR}_{x_i,l_i}^{\text{MRC}}\text{SIR}_{x_i,l_i'}^{\text{MRC}}\right] - (\overline{\text{SIR}}_{x_i,l_i}^{\text{MRC}})^2}{\text{Var}\left(\text{SIR}_{x_i,l_i}^{\text{MRC}}\right)}, \quad (8)$$

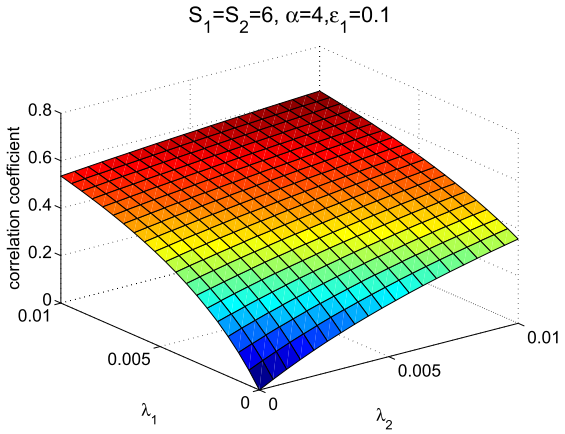

Fig. 4. Correlation coefficient *vs.* λ_1 and λ_2, where $K = 2$, $N^r = 8$, $x_i = 20$, $P_1 = 50$W, and $P_2 = 10$W.

where $\mathbb{E}[.]$ is the expectation operator, $\overline{\text{SIR}}_{x_i,l_i}^{\text{MRC}}$ is the average SIR value on data stream l_i, and Var[.] is the variance operator. The focus in the related literature (e.g., [16], [37]) is often on understanding of the interference correlation among antennas. In contrast, as [35] we here focus on the SIR correlation among data streams.

Proposition 2: For a typical UE receiving data from BS, x_i, in a MIMO-MRC multiplexing system, the correlation coefficient between data streams l_i and l_i', $\forall l_i, l_i', l_i \neq l_i'$ is given by Eq. (10), shown on the bottom of the next page, where $\check{\alpha} = 2/\alpha$, $\Lambda \triangleq \tilde{C}(\alpha)\sum_j \lambda_j \left(\frac{P_j}{S_j}\right)^{\check{\alpha}} \frac{\Gamma(\check{\alpha}+S_j)}{\Gamma(S_j)}$, $\tilde{C}(\alpha) \triangleq \pi\,\Gamma(1-\check{\alpha})$, $\Gamma(a) \triangleq \int_0^\infty e^{-z}z^{a-1}dz$, and

$$\overline{W}_j(t,\tau) \triangleq \int_0^\infty\int_0^\infty (tg_1 + \tau g_2)^{\check{\alpha}} \frac{(g_1 g_2)^{S_j-1}}{\Gamma^2(S_j)} e^{-(g_1+g_2)} dg_1 dg_2. \quad (9)$$

Proof: See Appendix B. ■

As shown in (10), the ICI affects the correlation coefficient mainly through Λ, where Λ is a function of BSs' density, their transmission powers and multiplexing gains, and the corresponding path-loss exponent. It is further shown in (10) that the multiplexing gains and CSI estimation inaccuracy may affect the correlation by imposing self-interference.

Fig. 4 shows the impact of λ_1 and λ_2 on $\rho_{x_i}^{\text{MRC}}(l_i, l_i')$. As it is seen for a sparse network, where $\lambda_1 \to 0$ and $\lambda_2 \to 0$,

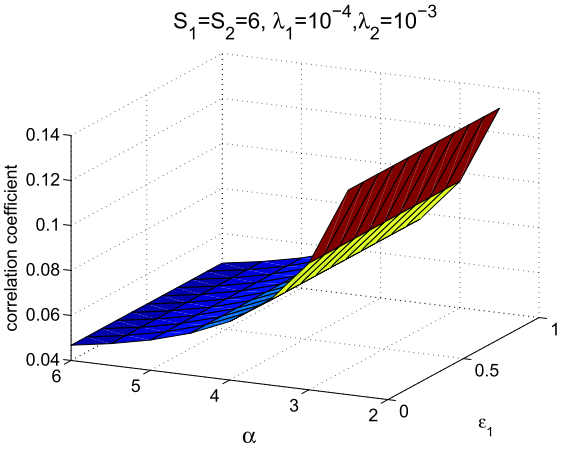

Fig. 5. Correlation coefficient *vs.* α and ϵ_1.

the correlation coefficient is very close to 0. In other words, the network behaves like an isolated link, where BSs are sparse in the coverage area. By increasing the density of BSs, however, $\rho_{x_i}^{\mathrm{MRC}}(l_i, l_i')$ is proportionally increased such that in an extreme case of high density of BSs where $\lambda_1 \approx 0.01$ and/or $\lambda_2 \approx 0.01$, the SIRs of data streams become highly correlated. In such a case, if a data stream, l_i, experiences outage due to a close-by interfering BS, then other data streams $l_i' \neq l_i$ will most likely experience the same.

Proposition 2 further shows that the imposed correlation due to the CSI estimation error seems negligible. This is because each individual data stream receives $S_i - 1$ inter-stream interference which is much more powerful than the interference imposed by the CSI estimation error. Fig. 5 confirms this, indicating that the SIR correlation is not affected by change in the value of ϵ_1.

The impact of path-loss exponent is also seen in Fig. 5. For a lower α, even a small number of moderately close interferers induce a substantial level of interference. This reduces the SIR for all data streams at the same time, thus causing a large correlation among data streams. For a higher value of α, the collective impact of the ICI received from the BSs located far from the receiver causes correlation, and hence unless the density of interferers is very high, the correlation is negligible.

One can therefore conclude that densification in multi-stream systems causes substantial SIR correlation among data streams through the ICI. This consequently affects the outage performance of the HetNet. Proposition 2, however, does not explicitly quantify the impact of the SIR correlation on the coverage performance.

B. Impact of SIR Correlation on the Coverage Performance

To analyze the impact of cross-stream SIR correlation on the coverage performance, here we introduce a multiplexing setting, namely *full-correlation* (FC) where the interference is fully correlated across all data streams in a link.[2] In other words, in the FC setting, the same level of ICI is received among all data streams in the communication link. Therefore, exchanging $G_{x_j,l_i}^{\mathrm{MRC}}$ with its average value, S_j, the ICI in the FC setting is $I^{\mathrm{FC}} = \sum_{j\in\mathcal{K}} \sum_{x_j\in\Phi_j/x_i} P_j \|x_j\|^{-\alpha}$. Assuming a typical UE is associated with BS x_i, the corresponding post-processing SIR for stream l_i is

$$\mathrm{SIR}_{x_i,l_i}^{\mathrm{MRC-FC}} = \frac{\frac{P_i}{S_i}\|x_i\|^{-\alpha}(1-\epsilon_i^2)H_{x_i,l_i}^{\mathrm{MRC}}}{\frac{P_i}{S_i\|x_i\|^{\alpha}}\left(\hat{H}_{x_i,l_i}^{\mathrm{MRC}} + \epsilon_i^2\tilde{H}_{x_i,l_i}^{\mathrm{MRC}}\right) + I^{\mathrm{FC}}}. \quad (11)$$

Based on the adopted CA policy, the associated BS for a link is the one that its corresponding smallest SIR values $\mathrm{SIR}_{x_i,l_i}^{\mathrm{MRC-FC}}$ across all data streams, is the maximum among all the BSs. Therefore, the typical UE is in coverage if

$$\mathcal{A}_{\mathrm{all}}^{\mathrm{MRC-FC}} = \left\{\exists i \in \mathcal{K} : \max_{x_i\in\Phi_i} \min_{l_i=1,\ldots,S_i} \mathrm{SIR}_{x_i,l_i}^{\mathrm{MRC-FC}} \geq \beta_i\right\}, \quad (12)$$

is not empty. An upper-bound on the corresponding coverage probability, $\mathcal{P}_C^{\mathrm{MRC-FC}}$, is given in the following proposition.

Proposition 3: In the FC setting, the coverage probability is upper-bounded as:

$$\mathcal{P}_C^{\mathrm{MRC-FC}} \leq \frac{\pi \sum_{i\in\mathcal{K}} \lambda_i \left(\frac{P_i(1-\epsilon_i^2)}{S_i^2\beta_i}\right)^{\breve{\alpha}} (\Theta(\beta_i,\epsilon_i,S_i))^{S_i}}{\tilde{C}(\alpha)\sum_{j=1}^{K}\lambda_j P_j^{\breve{\alpha}}}. \quad (13)$$

Proof: We prove the proposition by following the same line of argument as in the proof of Proposition 1. In the FC setting, (17) is reduced to

$$\mathcal{P}_C^{\mathrm{MRC-FC}} = \sum_{i\in\mathcal{K}} 2\pi\lambda_i \int_0^{\infty} x_i \mathbb{E}_{\{I^{\mathrm{FC}}\}} \prod_{l_i=1}^{S_i} \mathbb{P}\left\{\mathrm{SIR}_{x_i,l}^{\mathrm{MRC-FC}} \geq \beta_i \middle| I^{\mathrm{FC}}\right\} dx_i$$

[2]In [38] a similar assumption made to quantify signal correlation of optimal-combining in SIMO ad hoc networks.

$$\rho_{x_i}^{\mathrm{MRC}}(l_i,l_i') = \frac{\int_0^{\infty}\int_0^{\infty} \frac{e^{-\tilde{C}(\alpha)\sum_j \lambda_j (\frac{P_j}{S_j})^{\breve{\alpha}} \overline{W}_j(t,\tau)}}{1+(t+\tau)\frac{P_i}{S_i}x_i^{-\alpha}} - \frac{e^{-(t^{\breve{\alpha}}+\tau^{\breve{\alpha}})\Lambda}}{(1+t\frac{P_i}{S_i}x_i^{-\alpha})(1+\tau\frac{P_i}{S_i}x_i^{-\alpha})}}{\left(1+t\frac{P_i}{S_i}\epsilon_i^2 x_i^{-\alpha}\right)\left(1+\tau\frac{P_i}{S_i}\epsilon_i^2 x_i^{-\alpha}\right)\left((1+t\frac{P_i}{S_i}x_i^{-\alpha})(1+\tau\frac{P_i}{S_i}x_i^{-\alpha})\right)^{S_i-2}} dt d\tau}{\int_0^{\infty}\int_0^{\infty}\left[\frac{\frac{N^r+1}{N^r}e^{-(t+\tau)^{\breve{\alpha}}\Lambda}}{\left(1+\frac{(t+\tau)P_i\epsilon_i^2}{S_i x_i^{\alpha}}\right)\left(1+\frac{(t+\tau)P_i}{S_i x_i^{\alpha}}\right)^{S_i-1}} - \frac{e^{-(t^{\breve{\alpha}}+\tau^{\breve{\alpha}})\Lambda}}{\left(1+\frac{tP_i}{S_i x_i^{\alpha}}\epsilon_i^2\right)\left(1+\frac{P_i\epsilon_i^2\tau}{S_i x_i^{\alpha}}\right)\left((1+\frac{tP_i}{S_i x_i^{\alpha}})(1+\frac{P_i\tau}{S_i x_i^{\alpha}})\right)^{S_i-1}}\right] dt d\tau}, \quad (10)$$

$$= \sum_{i\in\mathcal{K}} 2\pi\lambda_i \int_0^\infty x_i \prod_{l_i=1}^{S_i} \int_0^\infty \frac{\mathcal{L}^{-1}_{\bar{\mathrm{F}}_{H_i^{\mathrm{MRC}}}}(t_i)}{\left(1+\frac{t_i\beta_i}{1-\epsilon_i^2}\right)^{S_i-1}(1+\frac{t_i\epsilon_i^2\beta_i}{1-\epsilon_i^2})} \times \prod_{j\in\mathcal{K}} \mathbb{E}_{\Phi_j} \prod_{x_j\in\Phi_j/x_i} e^{-t_i \frac{\beta_i S_i x_i^\alpha}{P_i(1-\epsilon_i^2)} P_j \|x_j\|^{-\alpha}} dt_i$$

$$\overset{(a)}{=} \sum_{i\in\mathcal{K}} 2\pi\lambda_i \int_0^\infty x_i \int_0^\infty \cdots \int_0^\infty \prod_{l_i=1}^{S_i} \frac{\mathcal{L}^{-1}_{\bar{\mathrm{F}}_{H_i^{\mathrm{MRC}}}}(t_{l_i})dt_{l_i}}{\left(1+\frac{t_{l_i}\beta_i}{1-\epsilon_i^2}\right)^{S_i-1}(1+\frac{t_{l_i}\epsilon_i^2\beta_i}{1-\epsilon_i^2})} \times e^{-x_i^2\tilde{C}(\alpha)\left(\frac{\beta_i S_i}{P_i(1-\epsilon_i^2)}\right)^{\breve{\alpha}} \sum_{j=1}^{K}\lambda_j P_j^{\breve{\alpha}} (\sum_{l_i=1}^{S_i} t_{l_i})^{\breve{\alpha}}}$$

$$\overset{(b)}{=} \frac{\pi}{\tilde{C}(\alpha)\sum_{j=1}^{K}\lambda_j P_j^{\breve{\alpha}}} \sum_{i\in\mathcal{K}} \lambda_i \left(\frac{\beta_i S_i}{P_i(1-\epsilon_i^2)}\right)^{-\breve{\alpha}} \int_0^\infty \cdots \int_0^\infty \times (\sum_{l_i=1}^{S_i} t_{l_i})^{-\breve{\alpha}} \prod_{l_i=1}^{S_i} \frac{\mathcal{L}^{-1}_{\bar{\mathrm{F}}_{H_i^{\mathrm{MRC}}}}(t_{l_i})}{\left(1+\frac{t_{l_i}\beta_i}{1-\epsilon_i^2}\right)^{S_i-1}(1+\frac{t_{l_i}\epsilon_i^2\beta_i}{1-\epsilon_i^2})} dt_{l_i}$$

$$\overset{(c)}{\leq} \frac{\pi}{\tilde{C}(\alpha)\sum_{j=1}^{K}\lambda_j P_j^{\breve{\alpha}}} \sum_{i\in\mathcal{K}} \lambda_i \left(\frac{\beta_i S_i^2}{P_i(1-\epsilon_i^2)}\right)^{-\breve{\alpha}} \int_0^\infty \cdots \int_0^\infty \times \prod_{l_i=1}^{S_i} \frac{t_{l_i}^{-\frac{\breve{\alpha}}{S_i}} \mathcal{L}^{-1}_{\bar{\mathrm{F}}_{H_i^{\mathrm{MRC}}}}(t_{l_i})}{\left(1+\frac{t_{l_i}\beta_i}{1-\epsilon_i^2}\right)^{S_i-1}(1+\frac{t_{l_i}\epsilon_i^2\beta_i}{1-\epsilon_i^2})} dt_{l_i}$$

$$\overset{(d)}{=} \frac{\pi}{\tilde{C}(\alpha)\sum_{j=1}^{K}\lambda_j P_j^{\breve{\alpha}}} \sum_{i\in\mathcal{K}} \lambda_i \left(\frac{\beta_i S_i^2}{P_i(1-\epsilon_i^2)}\right)^{-\breve{\alpha}} \prod_{l_i=1}^{S_i} \times \int_0^\infty \frac{t_{l_i}^{-\frac{\breve{\alpha}}{S_i}} \mathcal{L}^{-1}_{\bar{\mathrm{F}}_{H_i^{\mathrm{MRC}}}}(t_{l_i})}{\left(1+\frac{t_{l_i}\beta_i}{1-\epsilon_i^2}\right)^{S_i-1}(1+\frac{t_{l_i}\epsilon_i^2\beta_i}{1-\epsilon_i^2})} dt_{l_i}$$

$$\overset{(e)}{=} \frac{\pi}{\tilde{C}(\alpha)\sum_{j=1}^{K}\lambda_j P_j^{\breve{\alpha}}} \sum_{i\in\mathcal{K}} \lambda_i \left(\frac{\beta_i S_i^2}{P_i(1-\epsilon_i^2)}\right)^{-\breve{\alpha}} \times \left(\int_0^\infty \frac{t_i^{-\frac{\breve{\alpha}}{S_i}} \mathcal{L}^{-1}_{\bar{\mathrm{F}}_{H_i^{\mathrm{MRC}}}}(t_i)}{\left(1+\frac{t_i\beta_i}{1-\epsilon_i^2}\right)^{S_i-1}(1+\frac{t_i\epsilon_i^2\beta_i}{1-\epsilon_i^2})} dt_i\right)^{S_i},$$

where in (a) we insert the Laplace transform of I^{FC} and in (b) the integrals are reordered and we integrate the inner integral with respect to x_i. In (c) arithmetic-geometric inequality is applied followed by (d) and (e) where the fading gains, $H^{\mathrm{MRC}}_{x_i,l_i}$, are i.i.d. Applying the result of Appendix A in (e), completes the proof. ■

Comparing Propositions 1 and 3, we note that in general for the FC setting, the coverage probability has a more simplified form. On the other hand, the upper-bound of the coverage performance of a MIMO-MRC HetNet system is (almost) always higher than the same system assuming the FC setting. This is because by noting that for $\frac{\breve{\alpha}}{S_i} \in (0,1)$, there holds $\frac{\Gamma(\frac{\breve{\alpha}}{S_i}+S_j)}{\Gamma(S_j)} \lesssim S_j^{\frac{\breve{\alpha}}{S_i}}$ [37]. Therefore, noticing that both (13) and (4) have the same nominator while the denominator of the former is larger than that of the latter, we obtain $\mathcal{P}_C^{\mathrm{MRC-FC}} \lesssim \mathcal{P}_C^{\mathrm{MRC}}$. Consequently, we can conclude that adding to the correlation among data streams of a communication link can reduce the coverage probability. Although this result is based on the derived upper-bounds on the coverage probabilities in (13) and (4), our simulation results in Section V confirm its credibility.

C. What If the Cross-Stream SIR Correlation Is Overlooked?

The above analysis shows that approximating a practical scenario based on the FC setting results in underestimation of the coverage probability. Another way to simplify the coverage analysis is to simply ignore the cross stream SIR correlation, i.e., statistically independent SIR values. We refer to this case as *no-correlation* (NC) setting. Starting from (17) and assuming the NC setting, the coverage probability in (17) is written as

$$\mathcal{P}_C^{\mathrm{MRC-NC}} = \sum_{i\in\mathcal{K}} 2\pi\lambda_i \int_0^\infty x_i \prod_{l_i=1}^{S_i} \mathbb{E}_\Phi \mathbb{P}\left\{\mathrm{SIR}^{\mathrm{MRC}}_{x_i,l_i} \geq \beta_i \middle| \Phi\right\} dx_i. \tag{14}$$

The coverage probability in (14) can then be written as:

$$\mathcal{P}_C^{\mathrm{MRC-NC}} = \sum_{i\in\mathcal{K}} 2\pi\lambda_i \int_0^\infty x_i \prod_{l_i=1}^{S_i} \int_0^\infty \frac{\mathcal{L}^{-1}_{\bar{\mathrm{F}}_{H_i^{\mathrm{MRC}}}}(t_i)}{\left(1+\frac{t_i\beta_i}{1-\epsilon_i^2}\right)^{S_i-1}(1+\frac{t_i\epsilon_i^2\beta_i}{1-\epsilon_i^2})} \times \prod_{j\in\mathcal{K}} \mathbb{E}_{\Phi_j} \prod_{x_j\in\Phi_j/x_i} \mathbb{E}_{G^{\mathrm{MRC}}_{x_j,l_i}} e^{-t_i \frac{\beta_i S_i x_i^\alpha}{P_i(1-\epsilon_i^2)} \frac{P_j G^{\mathrm{MRC}}_{x_j,l_i}}{S_j\|x_j\|^\alpha}} dt_i$$

$$\overset{(a)}{=} \sum_{i\in\mathcal{K}} 2\pi\lambda_i \int_0^\infty x_i \int_0^\infty \cdots \int_0^\infty e^{-x_i^2\Lambda\left(\frac{\beta_i S_i}{P_i(1-\epsilon_i^2)}\right)^{\breve{\alpha}} (\sum_{l_i=1}^{S_i} t_{l_i}^{\breve{\alpha}})} \times \prod_{l_i=1}^{S_i} \frac{\mathcal{L}^{-1}_{\bar{\mathrm{F}}_{H_i^{\mathrm{MRC}}}}(t_{l_i})}{\left(1+\frac{t_{l_i}\beta_i}{1-\epsilon_i^2}\right)^{S_i-1}(1+\frac{t_{l_i}\epsilon_i^2\beta_i}{1-\epsilon_i^2})} dt_{l_i}$$

$$= \frac{\pi}{\Lambda} \sum_{i\in\mathcal{K}} \lambda_i \left(\frac{\beta_i S_i}{P_i(1-\epsilon_i^2)}\right)^{-\breve{\alpha}} \int_0^\infty \cdots \int_0^\infty \left(\prod_{l_i=1}^{S_i} t_{l_i}\right)^{-\breve{\alpha}} \times \prod_{l_i=1}^{S_i} \frac{\mathcal{L}^{-1}_{\bar{\mathrm{F}}_{H_i^{\mathrm{MRC}}}}(t_{l_i})}{\left(1+\frac{t_{l_i}\beta_i}{1-\epsilon_i^2}\right)^{S_i-1}(1+\frac{t_{l_i}\epsilon_i^2\beta_i}{1-\epsilon_i^2})} dt_{l_i}$$

$$= \frac{\pi}{\Lambda} \sum_{i\in\mathcal{K}} \lambda_i \left(\frac{\beta_i S_i^2}{P_i(1-\epsilon_i^2)}\right)^{-\breve{\alpha}} \prod_{l_i=1}^{S_i}$$

$$\times \int_0^\infty \frac{t_{l_i}^{-\breve{\alpha}} \mathcal{L}^{-1}_{\bar{\mathrm{F}}_{H_i^{\mathrm{MRC}}}}(t_{l_i}) dt_{l_i}}{\left(1+\frac{t_{l_i}\beta_i}{1-\epsilon_i^2}\right)^{S_i-1}(1+\frac{t_{l_i}\epsilon_i^2\beta_i}{1-\epsilon_i^2})}$$

$$\overset{(b)}{=} \frac{\pi}{\Lambda}\sum_{i\in\mathcal{K}}\lambda_i\left(\frac{\beta_i S_i^2}{P_i(1-\epsilon_i^2)}\right)^{-\breve{\alpha}} \times \left(\int_0^\infty \frac{t_i^{-\breve{\alpha}}\mathcal{L}^{-1}_{\bar{\mathrm{F}}_{H_i^{\mathrm{MRC}}}}(t_i)}{\left(1+\frac{t_i\beta_i}{1-\epsilon_i^2}\right)^{S_i-1}(1+\frac{t_i\epsilon_i^2\beta_i}{1-\epsilon_i^2})}dt_i\right)^{S_i},$$

where in (a) we insert the Laplace transform of the ICI and further notice the definition of Λ as in Proposition 2. Denoting the integral in (b) by $\tilde{\Theta}(\beta_i,\epsilon_i,S_i)$ and following the same line of argument as in Appendix A, we evaluate this integral as

$$\tilde{\Theta}(\beta_i,\epsilon_i,S_i) \triangleq \sum_{r_i=0}^{N^r-1}\sum_{q_i=0}^{r_i}\sum_{p_i=0}^{q_i}\frac{(-1)^{q_i-p_i}\beta_i^{2q_i-p_i}}{\epsilon_i^{-4q_i+2p_i}(1-\epsilon_i^2)^{S_i}} \times\frac{\left(1-\epsilon_i^2+\beta_i\right)^{-q_i-S_i+1}\left(1+\epsilon_i^2(\beta_i-1)\right)^{-q_i+p_i-1}}{p_i\mathrm{B}(S_i-1,p_i)(r_i-q_i)\mathrm{B}(\breve{\alpha},r_i-q_i)}. \tag{15}$$

Using this, (14) is then reduced to

$$\mathcal{P}_C^{\mathrm{MRC-NC}} = \frac{\pi}{\Lambda}\sum_{i\in\mathcal{K}}\lambda_i\left(\frac{P_i(1-\epsilon_i^2)}{S_i\beta_i}\right)^{\breve{\alpha}}\left(\tilde{\Theta}(\beta_i,\epsilon_i,S_i)\right)^{S_i}. \tag{16}$$

Note that NC setting is in fact an extreme case and thus $\mathcal{P}_C^{\mathrm{MRC-NC}}$ is not practically achievable. This is simply because it does not comply with the max-SIR CA rule as in the NC setting, an independent set of interferers appears on each data stream. Therefore, there might be cases where the typical UE becomes associated with different BSs for different data streams. This, however, contradicts the reality of the MIMO signal model as presented in 1.

We further note that, as $\breve{\alpha}\in(0,1)$, by using $\frac{\Gamma(\breve{\alpha}+S_j)}{\Gamma(S_j)}\lesssim S_j^{\breve{\alpha}}$ a lower-bound on $\mathcal{P}_C^{\mathrm{MRC-NC}}$ is

$$\mathcal{P}_C^{\mathrm{MRC-NC}} \gtrsim \frac{\pi\sum_{i\in\mathcal{K}}\lambda_i\left(\frac{P_i(1-\epsilon_i^2)}{S_i^2\beta_i}\right)^{\breve{\alpha}}\left(\tilde{\Theta}(\beta_i,\epsilon_i,S_i)\right)^{S_i}}{\tilde{C}(\alpha)\sum_{j=1}^K\lambda_j P_j^{\breve{\alpha}}} \geq \frac{\pi\sum_{i\in\mathcal{K}}\lambda_i\left(\frac{P_i(1-\epsilon_i^2)}{S_i^2\beta_i}\right)^{\breve{\alpha}}(\Theta(\beta_i,\epsilon_i,S_i))^{S_i}}{\tilde{C}(\alpha)\sum_{j=1}^K\lambda_j P_j^{\breve{\alpha}}} = \mathcal{P}_C^{\mathrm{MRC-FC}},$$

where the second inequality is because $\tilde{\Theta}(\beta_i,\epsilon_i,S_i)\geq\Theta(\beta_i,\epsilon_i,S_i)$. To confirm this, we notice that the beta function is a decreasing function of its argument, and observing that by comparing $\tilde{\Theta}(\beta_i,\epsilon_i,S_i)$ in (15) and $\Theta(\beta_i,\epsilon_i,S_i)$ in (7), we note that for a given positive number a, $\tilde{\Theta}(\beta_i,\epsilon_i,S_i)-\Theta(\beta_i,\epsilon_i,S_i)\propto\frac{1}{\mathrm{B}(\breve{\alpha},a)}-\frac{1}{\mathrm{B}(\frac{\breve{\alpha}}{S_i},a)}$.

On the other hand, since $\frac{\breve{\alpha}}{S_i}\in(0,1)$, there holds $\frac{\Gamma(\frac{\breve{\alpha}}{S_i}+S_j)}{\Gamma(S_j)}>S_j^{\frac{\breve{\alpha}}{S_i}}\Gamma(1+\frac{\breve{\alpha}}{S_i})$ [37]. Applying this, $\mathcal{P}_C^{\mathrm{MRC}}$ in (4) is further upper-bounded as

$$\mathcal{P}_C^{\mathrm{MRC}} \leq \frac{\pi\sum_{i\in\mathcal{K}}\lambda_i\left(\frac{P_i(1-\epsilon_i^2)}{S_i^2\beta_i}\right)^{\breve{\alpha}}\left(\Theta(\beta_i,\epsilon_i,S_i)\Gamma(1+\frac{\breve{\alpha}}{S_i})\right)^{S_i}}{\tilde{C}(\alpha)\sum_{j=1}^K\lambda_j P_j^{\breve{\alpha}}} \leq \frac{\pi\sum_{i\in\mathcal{K}}\lambda_i\left(\frac{P_i(1-\epsilon_i^2)}{S_i^2\beta_i}\right)^{\breve{\alpha}}(\Theta(\beta_i,\epsilon_i,S_i)))^{S_i}}{\tilde{C}(\alpha)\sum_{j=1}^K\lambda_j P_j^{\breve{\alpha}}} \leq \mathcal{P}_C^{\mathrm{MRC-NC}},$$

where the last line is because $\Gamma(1+\frac{\breve{\alpha}}{S_i})\leq 1$ for $\frac{\breve{\alpha}}{S_i}\in(0,1)$. Consequently, using the NC setting, the coverage probability is basically overestimated. This implies that the common approach that focuses on either isolated scenarios or non-isolated scenarios but with emphasis of the characterization of MIMO communications from the perspective of a data stream is essentially overestimation of the actual performance of the network.

V. Simulation Results

In this section, we use simulations to evaluate the performance of a MIMO-MRC HetNet setting and further examine the accuracy of the developed analysis. The simulated system is a 2-tier HetNet, i.e., $K=2$. The macro BS in the first tier has a high Tx power of $P_1=50$W. The second tier consists of femto BSs with a low Tx power of $P_2=1$W. The path-loss exponent is $\alpha=4$, and the CSI estimation error $\epsilon_i=0.1\ \forall i$, $N_1^t=N_2^t=16$. In a disk with radius $10,000$ units, we randomly drop BSs of each tier according to the corresponding tier densities. We set $\lambda_U=1$ so all the BSs are assumed to be active. We apply Monte Carlo technique and analyze $40,000$ snapshots of simulations. In each snapshot the MIMO channels are randomly generated. For the UEs, the corresponding SIR values are then calculated based on the MRC receiver.

A. Impact of Path-Loss Exponent, CSI Estimation Error, and SIR Threshold

Fig. 6.a shows the coverage probability *vs.* the estimation error, $\epsilon=\epsilon_i\ \forall i$, for several values of the path-loss exponent, α. The bound obtained in Prop. 1 is shown to be close to the simulation result. Also, increasing the CSI inaccuracy is shown to reduce the coverage performance. This is because the interference on each data stream is increased due to the CSI inaccuracy. It is also seen in Fig. 6.a that increasing the path-loss exponent improves the outage performance. Noting that a larger α implies a smaller signal strength, the improved outage performance suggests that the ICI is the main limiting factor.

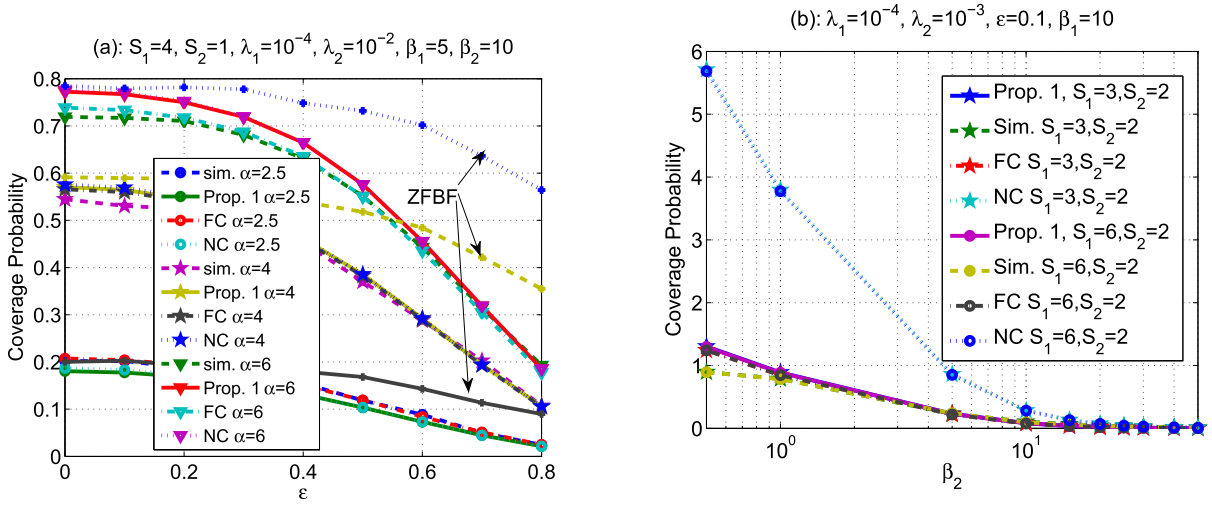

Fig. 6. (a): Coverage Probability *vs.* the CSI estimation error. (b): Coverage Probability *vs.* β_2.

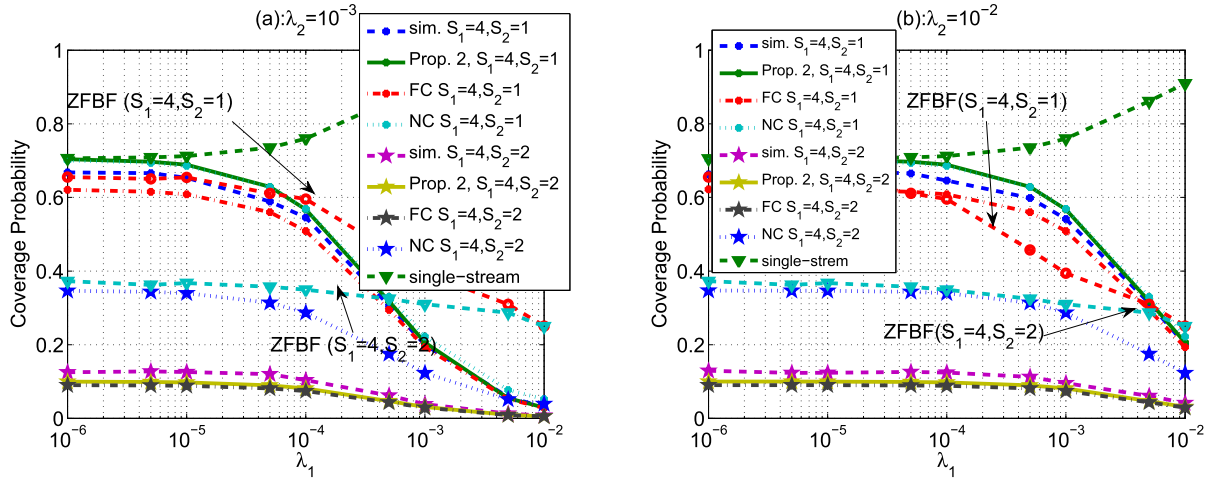

Fig. 7. (a): Coverage Probability *vs.* λ_1 when $\lambda_2 = 10^{-3}$; (b): Coverage Probability *vs.* λ_1 when $\lambda_2 = 10^{-2}$, where $\beta_1 = 5$, $\beta_2 = 10$, and $N^r = 10$.

Fig. 6.a also shows that in contrast to the cases with a smaller path-loss exponent (e.g., outdoor communications), the coverage is not significantly affected by the CSI inaccuracy where the path-loss exponent is high (e.g., indoor communications). This suggests that a simpler transceiver design or/and signaling protocol can be used without any significant compromise of the coverage probability. Fig. 6.b shows the coverage probability versus β_2. The bound obtained in Prop. 1 is is shown to be sufficiently accurate even for small values of β_2. It also shows that a higher β_2 results in a lower coverage performance.[3]

[3]When $\beta_i > 1$, the coverage probability is (almost) accurately (see [26] for more details) equivalent to the probability of whether or not there is a BS that can support the typical UE with the required SIR threshold [6]. However, for the case of $\beta_i < 1$ this may not be valid. Let $X = \sum_i \sum_{x_i \in \Phi_i} 1(\min_{l_i=1,\ldots,S_i} \mathrm{SIR}^{\mathrm{MRC}}_{x_i,l_i})$ denote the number of BSs that can support the typical UE, which is a Poisson random variable with mean value $\mu = \mathbb{E}[X]$. Thus, $P\{X > 1\} = 1 - \mu e^{-\mu} - e^{-\mu}$. For the case of Proposition 1 as well as FC assumption, our numerical results show that for $\mu \in [0, 1]$, $P\{X > 1\}$ is fairly small even when $0.2 < \beta_i < 1$, indicating our analysis under the assumption of $\beta_i \geq 1$ remains applicable. Nevertheless, for the case of NC, this probability becomes very large even when $\beta_i > 1$. We also expected this (see Section IV-C); since the NC assumption does not essentially provide the coverage probability as opposed to the reality of MIMO systems, it allows the typical UE to connect to different BSs for different data streams.

B. Impact of Densification and Multiplexing Gains

In Figs. 7 and 8 the coverage probability is given versus λ_1. We consider 5 settings (Stg) of multiplexing gains between two tiers, where Stg1, Stg2, Stg3, Stg4, and Stg5, respectively, refer to $(S_1 = 1, S_2 = 1)$, $(S_1 = 4, S_2 = 1)$, $(S_1 = 4, S_2 = 2)$, $(S_1 = 1, S_2 = 2)$, and $(S_1 = 8, S_2 = 2)$. Fig. 7 shows the coverage performance for Stg1, Stg2, and Stg3. The results of Stg1, Stg4, and Stg5 are plotted in Fig. 8. Both figures show the outage performance for $\lambda_2 = 10^{-3}$, and $\lambda_2 = 10^{-2}$.

It is seen in Figs. 7 and 8 that the analytical result presented in Prop. 1 closely follows the simulation results. It is also observed that a single stream communications, Stg1, generally outperforms the other combinations of multiplexing gains, regardless of the density of the BSs in both tiers. For the single stream case, it is also seen that densification in tier 1 always results in a higher improvement in the coverage probability. Nevertheless, comparison of Fig. 7.a with Fig. 7.b (resp. Fig. 8.a with Fig. 8.b) suggests that the improvement of the coverage probability by increasing λ_1 is reduced if tier 2 is also densified at the same time.

Fig. 7 also shows that for a small to moderate λ_1, increasing S_1 from 1 to 4 (Stg1→ Stg2) does not compromise coverage performance. However, for a sufficiently large λ_1, the coverage performance in Stg2 is significantly reduced.

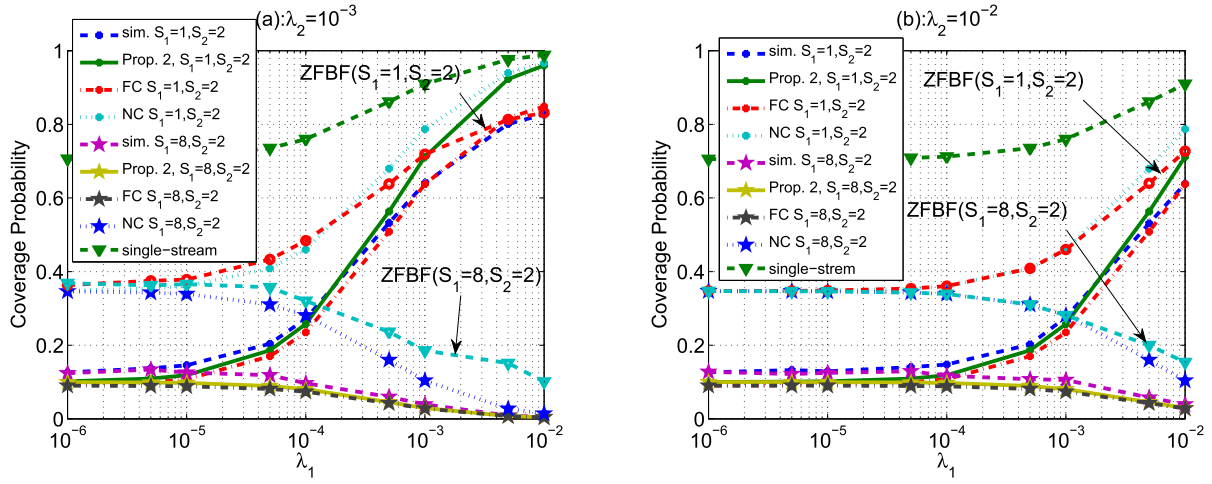

Fig. 8. (a): Coverage Probability *vs.* λ_1 when $\lambda_2 = 10^{-3}$; (b): Coverage Probability *vs.* λ_1 when $\lambda_2 = 10^{-2}$, where $\beta_1 = 5$, $\beta_2 = 10$, and $N^r = 10$.

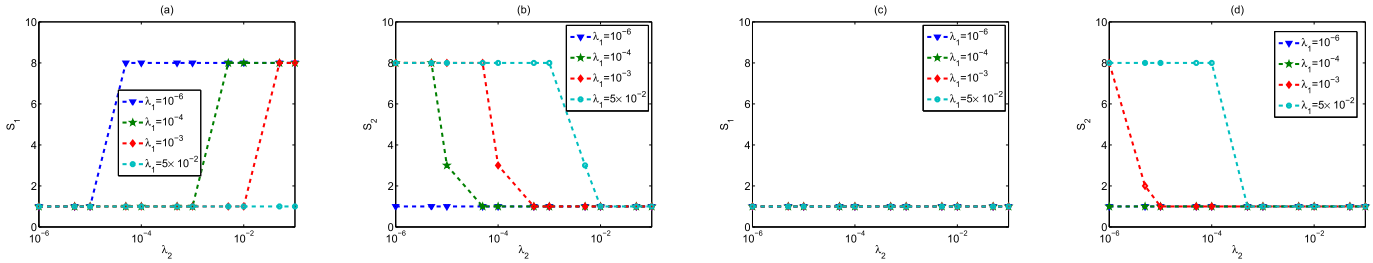

Fig. 9. (a): S_1, *vs.* λ_2 when $\epsilon_i = \epsilon = 0.1$; (b): S_2, *vs.* λ_2 when $\epsilon_i = \epsilon = 0.1$; (c): S_1, *vs.* λ_2 when $\epsilon_i = \epsilon = 0.25$; (d): S_2, *vs.* λ_2 when $\epsilon_i = \epsilon = 0.25$.

Comparing Fig. 7.a with Fig. 7.b, we further observe that for a higher value of λ_2, the positive impact of having a larger S_1 on the coverage performance is lower. Therefore, densification in tier 2 allows the growth of multiplexing gain in tier 1. This is because for a larger λ_2, the UEs are more likely to be associated with the BSs in tier 2. This is because the successful decoding of a data streams where $S_2 = 1$ is more probable than that of $S_1 = 4$, so the coverage probability is improved.

Results in Fig. 8 show that for a small to moderate λ_1, increasing S_2 from 1 to 2 (Stg1→ Stg4) substantially reduces the coverage performance. To tackle this problem, one may consider increasing λ_1 which reduces the performance gap. For a very dense tier 1, the coverage performance of Stg1 and Stg4 are then converged. Comparing Fig. 8.a with Fig. 8.b, one can see that by increasing λ_2, the impact of S_2 on the coverage performance is increased. Therefore, when densifying tier 2, increasing its multiplexing gain is not recommended. This is because for a larger λ_2, the UEs are more likely to be associated with the BSs in tier 2. The chance of successful decoding of $S_2 = 2$ is less than that of $S_2 = 1$, and hence the coverage probability is reduced. To address this issue, one might densify tier 1. By increasing λ_1, UEs are more often associated with the BSs in tier 1, where $S_1 = 1$ and it is more likely for the data stream to be successfully decoded.

It is further seen in Figs. 7 and 8 that both Stg3 and Stg4 similarly perform with a low coverage performance, where densification neither in tier 1 nor in tier 2, can compensate the significant coverage reduction compared to Stg1. This is because in cases where both S_1 and S_2 are high, successful decoding of data streams is less likely, even for a high density of the BSs. For such cases, reducing the multiplexing gains seems the only way to improve the coverage performance.

The above discussions suggest that increasing the multiplexing gains may compromise the coverage performance. Here, we investigate whether or not one can increase multiplexing gains in MRC without compromising the coverage performance compared to a single-stream system (SIMO). We derive the best combinations of multiplexing gains S_1 and S_2 that guarantee $\mathcal{P}_C^{\text{SIMO}} - \mathcal{P}_C^{\text{MRC}} < \xi_3$, where $\xi_3 \in (0, 1)$ is a given threshold:

$$O_2: \max_{S_1,S_2}(S_1 + S_2), \quad s.t.\ \mathcal{P}_C^{\text{SIMO}} - \mathcal{P}_C^{\text{MRC}} \leq \xi_3.$$

This optimization provides the maximum number of data streams across tiers, subject to an acceptable level of coverage degradation compared to SIMO. In Figs. 9.a and 9.b for ($\epsilon_i = \epsilon = 0.1\ \forall i$) (lower inaccuracy level), and Figs.9.c and 9.d for ($\epsilon_i = \epsilon = 0.25, \forall i$) (higher inaccuracy level), we derive the optimal values for several values of deployment densities where $\zeta_3 = 0.05$. For $\epsilon_i = \epsilon = 0.1$, Figs. 9.a and 9.b show that multi-stream MIMO communications with large multiplexing gains across tiers can be adopted without degrading the coverage probability compared to SIMO. It is, however, important to carefully select the multiplexing gains in each tier according to deployment densities. For instance, Fig. 9.a implies that by increasing λ_2 it is possible to increase S_1, but by densification of tier 1, a smaller S_1 should be selected. Therefore, a large S_1 is suitable only when tier 2 is highly densified. Fig. 9.b also shows that simultaneous densification and increasing multiplexing in tier 2 compromise the coverage probability. Similarly, with densification in tier 1, one should select a smaller multiplexing gain in tier 2.

We then conclude that by increasing the multiplexing gain in a tier, the coverage performance might be compromised, and thus densification in the other tier is required to preserve the coverage performance. This is because by increasing the multiplexing gain of a tier, it becomes harder to preserve the required coverage performance. Therefore, the potential coverage loss needs to be compensated through densification in the other tier while keeping its multiplexing gain as small as possible such that a larger number of UEs is getting associated with this tier. We then provide a simple rule of thumb which suggests densification of the tiers with lower multiplexing gains, and let the tiers with lower density transmit a larger number of data streams.

We further consider the cases with a higher level of CSI inaccuracy ($\epsilon_i = \epsilon = 0.25$), see Figs. 9.c and 9.d. Comparison of Figs. 9.a and 9.b shows that increasing the level of CSI inaccuracies reduces the suitability of multi-stream communications. Fig. 9.c also indicates that there is no setting for which multi-stream communications in tier 1 improves the coverage while according to Fig. 9.d, tier 2 can have multi-stream communications. Consistently with the low-level inaccuracy, we also observed that a simultaneous increase of λ_2 and S_2 does not improve coverage.

C. Impact of the SIR Correlation

In Section IV we quantitatively investigated the impact of SIR correlation on the coverage probability. We show that under FC setting the upper-bound of the coverage probability is underestimated, whereas by ignoring SIR correlation, the coverage probability is overestimated. These results in Figs 6, 7, and 8 confirmed the above analysis.

We further observe that the coverage probability in the NC setting *substantially* overestimates the coverage performance, while surprisingly the FC setting *slightly* underestimates the coverage performance. From Fig. 6.a we also notice that for a smaller α, the coverage probability in the FC setting becomes more accurate for the same reason as the observation made in Fig. 5, where a smaller path-loss exponent results in a larger SIR correlation.

D. Comparison With ZFBF

Fig. 6.a plots the coverage performance of ZFBF versus the level of CSI inaccuracy ϵ. ZFBF is, in general, shown to be more resilient to CSI inaccuracy than that of MRC. However, for small to moderate CSI inaccuracy, both systems perform almost the same, while MRC has a much lower computational complexity. Furthermore, as shown in Figs. 7 and 8, there exist combinations of multiplexing gains and deployment densities in which, compared to MRC, ZFBF does not improve coverage performance, see, e.g., Fig. 7.a for $(S_1, S_2) = (4, 1)$ where $\lambda_1 < 10^{-4}$, and Fig. 8.a for $(S_1, S_2) = (1, 2)$ where $\lambda_1 > 10^{-3}$. In such cases, it would be preferable to use the latter.

VI. Conclusion

Adopting tools of stochastic geometry, we studied the coverage probability of MIMO-MRC multiplexing systems in HetNets. Our analysis incorporated impacts of many important system parameters including the density of BSs, transmission powers, SIR thresholds, multiplexing gains, and CSI inaccuracies on the coverage performance. We derived an accurate upper-bound on the coverage probability in a closed-form. Important engineering insights were derived from scrutinizing our analytical and simulation results: (*i*) densification in multiplexing systems will be practiced in conjunction with multiplexing gains, else dramatic coverage loss might be inevitable; (*ii*) in indoor scenarios (high path-loss exponent regimes) it is possible to reduce the pilot signaling overhead designated for CSI estimation without imposing noticeable coverage loss; (*iii*) although MRC suffers from intra-stream interference in comparison to more complex receivers such as ZFBF, the relative coverage loss in large array scenarios and/or for cell edge users is barely noticeable.

We also developed analytical tools facilitating thorough investigations of the impacts of cross-stream SIR correlation on the coverage performance of multi-stream systems. Specifically, by focusing on the communication scenarios that the successful decoding of all transmitted data streams are required for the coverage, assuming full correlation among data streams is shown to yield a slightly smaller coverage performance. On the other hand, our analysis proved that by neglecting such correlation, as commonly assumed in the literature, one should expect a substantial overestimation of the coverage probability.

The results in this paper can be further utilized for performance bench-marking, where the performance of advanced MIMO techniques is compared to zero-feedback MRC. Such a comparison provides quantitative insights on the cost versus the benefit of adopting such techniques, e.g., the higher computational complexities and the required signaling overheads versus the gain on the coverage. Besides, our results provide an analytical tool for designing system parameters and aspects such as the required CSI accuracy and network coverage performance based on the wireless environment characteristics, such as path-loss exponent.

Appendix A
Proof of Proposition 1

We use [6, Lemma 1] and note that $\beta_i \geq 1$, $\forall i$, and write

$$\begin{aligned}\mathcal{P}_C^{\mathrm{MRC}} &= \sum_{i\in\mathcal{K}} \mathbb{E} \sum_{x_i\in\Phi_i} 1\left(\min_{l_i=1,\ldots,S_i} \mathrm{SIR}_{x_i,l_i}^{\mathrm{MRC}} \geq \beta_i\right) \\ &= \sum_{i\in\mathcal{K}} 2\pi\lambda_i \int_0^\infty x_i \mathbb{E}_{\{\Phi_j\}} \mathbb{P}\left\{\mathrm{SIR}_{x_i,l_i}^{\mathrm{MRC}} \geq \beta_i : \forall l_i \middle| \{\Phi_j\}\right\} dx_i \\ &= \sum_{i\in\mathcal{K}} 2\pi\lambda_i \int_0^\infty x_i \mathbb{E}_{\{\Phi_j\}} \prod_{l_i=1}^{S_i} \mathbb{P}\left\{\mathrm{SIR}_{x_i,l}^{\mathrm{MRC}} \geq \beta_i \middle| \{\Phi_j\}\right\} dx_i,\end{aligned} \tag{17}$$

where the first equation is according to Slivnyak- and Campbell-Mecke's Theorems [40]. We then note that conditioned to processes Φ_js, the SIR values across streams are statistically independent. For a fixed value of x_i, we have

$$\begin{aligned}&\mathbb{P}\left\{\mathrm{SIR}_{x_i,l_i}^{\mathrm{MRC}} \geq \beta_i \middle| \{\Phi_j\}\right\} \\ &\quad = \mathbb{P}\left\{H_{x_i,l_i}^{\mathrm{MRC}} \geq \frac{\beta_i(\epsilon_i^2 \tilde{H}_{x_i,l_i}^{\mathrm{MRC}} + \hat{H}_{x_i,l_i}^{\mathrm{MRC}})}{1-\epsilon_i^2} + \frac{S_i \beta_i x_i^\alpha}{P_i(1-\epsilon_i^2)}\right.\end{aligned}$$

$$\times \sum_{j\in\mathcal{K}} \sum_{x_j\in\Phi_j/x_i} \frac{P_j}{S_j}\|x_j\|^{-\alpha} G^{\mathrm{MRC}}_{x_j,l_i} \big| \{\Phi_j\}\Big\}$$

$$= \int_0^\infty \mathcal{L}^{-1}_{\bar{\mathrm{F}}_{H_i^{\mathrm{MRC}}}}(t_i)\mathbb{E} e^{-t_i \frac{\beta_i(\epsilon_i^2 \tilde{H}^{\mathrm{MRC}}_{x_i,l_i} + \hat{H}^{\mathrm{MRC}}_{x_i,l_i})}{1-\epsilon_i^2}}$$

$$\times \prod_{j\in\mathcal{K}} \prod_{x_j\in\Phi_j/x_i} \mathbb{E}_{G^{\mathrm{MRC}}_{x_j,l_i}} e^{-t_i \frac{\beta_i S_i x_i^\alpha}{P_i(1-\epsilon_i^2)} \frac{P_j}{S_j}\|x_j\|^{-\alpha} G^{\mathrm{MRC}}_{x_j,l_i}} dt_i$$

$$= \int_0^\infty \frac{\mathcal{L}^{-1}_{\bar{\mathrm{F}}_{H_i^{\mathrm{MRC}}}}(t_i)}{\left(1+\frac{t_i\beta_i}{1-\epsilon_i^2}\right)^{S_i-1}(1+\frac{t_i\epsilon_i^2\beta_i}{1-\epsilon_i^2})}$$

$$\times \prod_{j\in\mathcal{K}} \prod_{x_j\in\Phi_j/x_i} \mathbb{E}_{G^{\mathrm{MRC}}_{x_j,l_i}} e^{-t_i \frac{\beta_i S_i x_i^\alpha}{P_i(1-\epsilon_i^2)} \frac{P_j}{S_j\|x_j\|^\alpha} G^{\mathrm{MRC}}_{x_j,l_i}} dt_i, \quad (18)$$

where $\mathcal{L}^{-1}_{\bar{\mathrm{F}}_{H_i^{\mathrm{MRC}}}}(t_i)$ is the inverse Laplace transform of H_i^{MRC}, $\mathcal{L}^{-1}_{\bar{\mathrm{F}}_{H_i^{\mathrm{MRC}}}}(t_i) = \sum_{m=0}^{N^r-1} \frac{1}{m!}\delta^{(m)}(t-1)$ (see, [36, Lemmas 1 and 2]), and $\delta^{(m)}(t)$ is the m-th derivative of the Dirac delta function. Note that in (18) we drop index l_i from $\mathcal{L}_{\bar{\mathrm{F}}_{H_i^{\mathrm{zf}}}}(t_i)$ because $H^{\mathrm{zf}}_{x_i,l_i}$ are identical random variables (rv.) across the streams. Substituting (18) into (17) followed by straightforward derivations yields

$$\mathcal{P}_C^{\mathrm{MRC}} = \sum_{i\in\mathcal{K}} 2\pi\lambda_i \int_0^\infty x_i \mathbb{E}_{\{\Phi_j\}}$$

$$\times \prod_{l_i=1}^{S_i} \int_0^\infty \frac{\mathcal{L}^{-1}_{\bar{\mathrm{F}}_{H_i^{\mathrm{MRC}}}}(t_i)dt_i dx_i}{\left(1+\frac{t_i\beta_i}{1-\epsilon_i^2}\right)^{S_i-1}(1+\frac{t_i\epsilon_i^2\beta_i}{1-\epsilon_i^2})}$$

$$\times \prod_{j\in\mathcal{K}} \prod_{x_j\in\Phi_j/x_i} \mathbb{E}_{G^{\mathrm{MRC}}_{x_j,l_i}} e^{-t_i \frac{\beta_i S_i x_i^\alpha}{P_i(1-\epsilon_i^2)} \frac{P_j}{S_j}\|x_j\|^{-\alpha} G^{\mathrm{MRC}}_{x_j,l_i}}$$

$$= \sum_{i\in\mathcal{K}} 2\pi\lambda_i \int_0^\infty x_i dx_i \mathbb{E}_\Phi \int_0^\infty \cdots \int_0^\infty$$

$$\times \prod_{l_i=1}^{S_i} \frac{\mathcal{L}^{-1}_{\bar{\mathrm{F}}_{H_i^{\mathrm{MRC}}}}(t_{l_i})dt_{l_i}}{\left(1+\frac{t_{l_i}\beta_i}{1-\epsilon_i^2}\right)^{S_i-1}(1+\frac{t_{l_i}\epsilon_i^2\beta_i}{1-\epsilon_i^2})}$$

$$\times \prod_{j\in\mathcal{K}} \prod_{x_j\in\Phi_j/x_i} \mathbb{E}_{G^{\mathrm{MRC}}_{x_j}} \prod_{l_i=1}^{S_i} e^{-\frac{\beta_i S_i x_i^\alpha}{P_i(1-\epsilon_i^2)} \frac{P_j G^{\mathrm{MRC}}_{x_j,l_i} t_{l_i}}{S_j\|x_j\|^\alpha}},$$

as rv.s $G^{\mathrm{zf}}_{x_j,l_i}$ are independent and identically distributed (i.i.d.) rv.s across the streams. Thus,

$$\mathcal{P}_C^{\mathrm{MRC}}$$

$$= \sum_{i\in\mathcal{K}} 2\pi\lambda_i \int_0^\infty x_i dx_i \int_0^\infty \cdots \int_0^\infty$$

$$\times \prod_{l_i=1}^{S_i} \frac{\mathcal{L}^{-1}_{\bar{\mathrm{F}}_{H_i^{\mathrm{MRC}}}}(t_i)dt_{l_i}}{\left(1+\frac{t_i\beta_i}{1-\epsilon_i^2}\right)^{S_i-1}(1+\frac{t_i\epsilon_i^2\beta_i}{1-\epsilon_i^2})}$$

$$\times \prod_{j\in\mathcal{K}} \mathbb{E}_{\Phi_j} \prod_{x_j\in\Phi_j/x_i} \mathbb{E}_{G^{\mathrm{MRC}}_{x_j}} e^{-\frac{\beta_i S_i x_i^\alpha}{P_i(1-\epsilon_i^2)} \frac{P_j \sum_{l_i=1}^{S_i} G^{\mathrm{MRC}}_{x_j,l_i} t_{l_i}}{S_j\|x_j\|^\alpha}}$$

$$= \sum_{i\in\mathcal{K}} 2\pi\lambda_i \int_0^\infty x_i dx_i \int_0^\infty \cdots \int_0^\infty \prod_{l_i=1}^{S_i} \frac{\mathcal{L}^{-1}_{\bar{\mathrm{F}}_{H_i^{\mathrm{MRC}}}}(t_i)dt_{l_i}}{\left(1+\frac{t_i\beta_i}{1-\epsilon_i^2}\right)^{S_i-1}(1+\frac{t_i\epsilon_i^2\beta_i}{1-\epsilon_i^2})}$$

$$\times e^{-x_i^2\tilde{C}(\alpha)\left(\frac{\beta_i S_i}{P_i(1-\epsilon_i^2)}\right)^{\breve{\alpha}} \sum_{j=1}^K \lambda_j \left(\frac{P_j}{S_j}\right)^{\breve{\alpha}} \mathbb{E}_{G_j^{\mathrm{MRC}}}\left[(\sum_{l_i=1}^{S_i} G^{\mathrm{MRC}}_{j,l_i} t_{l_i})^{\breve{\alpha}}\right]}$$

Reordering the integrals we then have

$$\mathcal{P}_C^{\mathrm{MRC}}$$

$$= \sum_{i\in\mathcal{K}} 2\pi\lambda_i \int_0^\infty \cdots \int_0^\infty \prod_{l_i=1}^{S_i} \frac{\mathcal{L}^{-1}_{\bar{\mathrm{F}}_{H_i^{\mathrm{MRC}}}}(t_i)dt_{l_i}}{\left(1+\frac{t_i\beta_i}{1-\epsilon_i^2}\right)^{S_i-1}(1+\frac{t_i\epsilon_i^2\beta_i}{1-\epsilon_i^2})}$$

$$\times \int_0^\infty x_i e^{-x_i^2\tilde{C}(\alpha)\left(\frac{\beta_i S_i}{P_i(1-\epsilon_i^2)}\right)^{\breve{\alpha}} \sum_{j=1}^K \lambda_j \left(\frac{P_j}{S_j}\right)^{\breve{\alpha}} \mathbb{E}\left[(\sum_{l_i=1}^{S_i} G^{\mathrm{MRC}}_{j,l_i} t_{l_i})^{\breve{\alpha}}\right]} dx_i$$

$$= \sum_{i\in\mathcal{K}} \frac{\pi}{\tilde{C}(\alpha)} \int_0^\infty \cdots \int_0^\infty \frac{\lambda_i \left(\frac{P_i(1-\epsilon_i^2)}{S_i\beta_i}\right)^{\breve{\alpha}}}{\sum_{j\in\mathcal{K}} \lambda_j \left(\frac{P_j}{S_j}\right)^{\breve{\alpha}} \mathbb{E}_{G_j^{\mathrm{MRC}}}\left[(\sum_{l_i=1}^{S_i} G^{\mathrm{MRC}}_{j,l_i} t_{l_i})^{\breve{\alpha}}\right]}$$

$$\times \prod_{l_i=1}^{S_i} \frac{\mathcal{L}^{-1}_{\bar{\mathrm{F}}_{H_i^{\mathrm{MRC}}}}(t_i)dt_{l_i}}{\left(1+\frac{t_i\beta_i}{1-\epsilon_i^2}\right)^{S_i-1}(1+\frac{t_i\epsilon_i^2\beta_i}{1-\epsilon_i^2})},$$

which is not easily tractable due to $\mathbb{E}_{G_j^{\mathrm{MRC}}}\big[(\sum_{l_i=1}^{S_i} G^{\mathrm{MRC}}_{j,l_i} t_{l_i})^{\breve{\alpha}}\big]$. To make the analysis tractable, we transform $\sum_{l_i=1}^{S_i} G^{\mathrm{MRC}}_{j,l_i} t_{l_i}$ into a multiplicative form $\prod_{l_i=1}^{S_i} G^{\mathrm{MRC}}_{j,l_i} t_{l_i}$ so that expectation operation on G^{MRC}_{j,l_i} becomes effective irrespective of variables t_{l_i}s. To do this, we adopt the arithmetic-geometric inequality, which results in the following upper-bound on the coverage probability:

$$\mathcal{P}_C^{\mathrm{MRC}} \le \sum_{i\in\mathcal{K}} \frac{\frac{\pi}{\tilde{C}(\alpha)} \left(\frac{P_i(1-\epsilon_i^2)}{S_i\beta_i}\right)^{\breve{\alpha}} \frac{\lambda_i}{S_i^{\breve{\alpha}}}}{\sum_{j=1}^K \lambda_j \left(\frac{P_j}{S_j}\right)^{\breve{\alpha}} \mathbb{E}_{G_j^{\mathrm{MRC}}} \prod_{l_i=1}^{S_i} (G^{\mathrm{MRC}}_{j,l_i})^{\frac{\breve{\alpha}}{S_i}}} \int_0^\infty \cdots \int_0^\infty$$

$$\times \prod_{l_i=1}^{S_i} \frac{t_{l_i}^{-\frac{\breve{\alpha}}{S_i}} \mathcal{L}^{-1}_{\bar{\mathrm{F}}_{H_i^{\mathrm{MRC}}}}(t_{l_i})}{\left(1+\frac{t_i\beta_i}{1-\epsilon_i^2}\right)^{S_i-1}(1+\frac{t_i\epsilon_i^2\beta_i}{1-\epsilon_i^2})} dt_{l_i}$$

$$= \sum_{i\in\mathcal{K}} \frac{\frac{\pi}{\tilde{C}(\alpha)}\left(\frac{P_i(1-\epsilon_i^2)}{S_i\beta_i}\right)^{\breve{\alpha}}\frac{\lambda_i}{S_i^{\breve{\alpha}}}}{\sum_{j=1}^{K}\lambda_j\left(\frac{P_j}{S_j}\right)^{\breve{\alpha}}\left(\mathbb{E}_{G_j^{\mathrm{MRC}}}(G_j^{\mathrm{MRC}})^{\frac{\breve{\alpha}}{S_i}}\right)^{S_i}} \times \left(\int_0^{\infty}\frac{t_i^{-\frac{\breve{\alpha}}{S_i}}\mathcal{L}^{-1}_{\bar{\mathrm{F}}_{H_i^{\mathrm{MRC}}}}(t_i)}{\left(1+\frac{t_i\beta_i}{1-\epsilon_i^2}\right)^{S_i-1}(1+\frac{t_i\epsilon_i^2\beta_i}{1-\epsilon_i^2})}\right)^{S_i}, \quad (19)$$

where the last step is due to the fact that rv.s $G^{\mathrm{MRC}}_{x_j,l_i}$ are i.i.d. across streams. We now evaluate the integral in (19). Using the characteristics of Dirac delta function, we write

$$\int_0^{\infty}\frac{t_i^{-\frac{\breve{\alpha}}{S_i}}\mathcal{L}^{-1}_{\bar{\mathrm{F}}_{H_i^{\mathrm{MRC}}}}(t_i)}{\left(1+\frac{t_i\beta_i}{1-\epsilon_i^2}\right)^{S_i-1}(1+\frac{t_i\epsilon_i^2\beta_i}{1-\epsilon_i^2})}dt_i$$
$$= \sum_{r_i=0}^{N^r-1}\frac{1}{r_i!}\int_0^{\infty}\delta^{(r_i)}(t_i-1)\frac{t_i^{-\frac{\breve{\alpha}}{S_i}}}{\left(1+\frac{t_i\beta_i}{1-\epsilon_i^2}\right)^{S_i-1}(1+\frac{t_i\epsilon_i^2\beta_i}{1-\epsilon_i^2})}dt_i$$
$$= \sum_{r_i=0}^{N^r-1}\frac{(-1)^{r_i}}{r_i!}\frac{d^{r_i}}{dt^{r_i}}\frac{t^{-\frac{\breve{\alpha}}{S_i}}}{\left(1+\frac{t_i\beta_i}{1-\epsilon_i^2}\right)^{S_i-1}(1+\frac{t_i\epsilon_i^2\beta_i}{1-\epsilon_i^2})}\Big|_{t=1}. \quad (20)$$

Applying the Leibniz rule along with straightforward mathematical derivation we then get

$$\frac{d^{r_i}}{dt^{r_i}}\frac{t^{-\frac{\breve{\alpha}}{S_i}}}{\left(1+\frac{t\beta_i}{1-\epsilon_i^2}\right)^{S_i-1}\left(1+\frac{t\epsilon_i^2\beta_i}{1-\epsilon_i^2}\right)}$$
$$= \sum_{q_i=0}^{r_i}\binom{r_i}{q_i}\frac{d^{q_i}}{dt^{q_i}}\frac{1}{\left(1+\frac{t\beta_i}{1-\epsilon_i^2}\right)^{S_i-1}}\frac{1}{\left(1+\frac{t\epsilon_i^2\beta_i}{1-\epsilon_i^2}\right)}\frac{d^{r_i-q_i}}{dt^{r_i-q_i}}t^{-\frac{\breve{\alpha}}{S_i}}$$
$$= \sum_{q_i=0}^{r_i}\binom{r_i}{q_i}\sum_{p_i=0}^{q_i}\binom{q_i}{p_i}\frac{d^{p_i}}{dt^{p_i}}\frac{1}{\left(1+\frac{t\beta_i}{1-\epsilon_i^2}\right)^{S_i-1}}$$
$$\times\frac{d^{q_i-p_i}}{dt^{q_i-p_i}}\frac{1}{\left(1+\frac{t\epsilon_i^2\beta_i}{1-\epsilon_i^2}\right)}\frac{d^{r_i-q_i}}{dt^{r_i-q_i}}t^{-\frac{\breve{\alpha}}{S_i}}. \quad (21)$$

which is

(21)

$$= \sum_{q_i=0}^{r_i}\sum_{p_i=0}^{q_i}\frac{\binom{r_i}{q_i}\binom{q_i}{p_i}\prod_{m_i=0}^{p_i-1}(S_i-1+m_i)}{(\frac{-\beta_i}{1-\epsilon_i^2})^{-q_i}\left(1+\frac{t\beta_i}{1-\epsilon_i^2}\right)^{q_i+S_i-1}} \times\frac{\prod_{u_i=0}^{q_i-p_i-1}(1+u_i)}{(\frac{-\beta_i\epsilon_i^2}{1-\epsilon_i^2})^{-q_i+p_i}\left(1+\frac{t\beta_i\epsilon_i^2}{1-\epsilon_i^2}\right)^{q_i-p_i+1}}\frac{\prod_{n_i=0}^{r_i-q_i-1}(\frac{\breve{\alpha}}{S_i}+n_i)}{(-1)^{-r_i+q_i}t^{\frac{\breve{\alpha}}{S_i}+r_i-q_i}}$$
$$= (-1)^{r_i}\sum_{q_i=0}^{r_i}\sum_{p_i=0}^{q_i}\frac{(-1)^{q_i-p_i}\binom{r_i}{q_i}\binom{q_i}{p_i}\Gamma(S_i-1+p_i)}{\epsilon_i^{2p_i-4q_i}\left(1+\frac{\beta_i}{1-\epsilon_i^2}\right)^{q_i+S_i-1}\left(\frac{\beta_i}{1-\epsilon_i^2}\right)^{p_i-2q_i}} \times\frac{\Gamma(q_i-p_i+1)\Gamma(\frac{\breve{\alpha}}{S_i}+r_i-q_i)}{\left(1+\frac{\beta_i\epsilon_i^2}{1-\epsilon_i^2}\right)^{q_i-p_i+1}\Gamma(S_i-1)\Gamma(\frac{\breve{\alpha}}{S_i})}.$$

Using this, (20) is then re written as

$$(20) = \sum_{r_i=0}^{N^r-1}\sum_{q_i=0}^{r_i}\sum_{p_i=0}^{q_i}\frac{(-1)^{q_i-p_i}\beta_i^{2q_i-p_i}}{\epsilon_i^{-4q_i+2p_i}} \times\frac{\left(1-\epsilon_i^2+\beta_i\right)^{-q_i-S_i+1}\left(1+\epsilon_i^2(\beta_i-1)\right)^{-q_i+p_i-1}}{(1-\epsilon_i^2)^{S_i}\,p_i\mathrm{B}(S_i-1,\,p_i)(r_i-q_i)\mathrm{B}(\frac{\breve{\alpha}}{S_i},r_i-q_i)}. \quad (22)$$

Finally, by substituting (22) into (19), and noticing that $G^{\mathrm{MRC}}_{x_j,l_i}$ is chi-squared with $2S_j$ DoFs, the desired result follows.

Appendix B
Proof of Proposition 2

We start with the evaluation of $\overline{\mathrm{SIR}}^{\mathrm{MRC}}_{x_i,l_i}$. Due to the independence of the intended and interfering signals, and noting that $H^{\mathrm{MRC}}_{x_i,l_i}$ is a chi-square distributed with $2N^r$ DoFs, we write

$$\overline{\mathrm{SIR}}^{\mathrm{MRC}}_{x_i,l_i} = \frac{P_iN^r(1-\epsilon_i^2)}{S_ix_i^{\alpha}}\mathbb{E}\Bigg(\frac{P_i}{S_ix_i^{\alpha}}(\epsilon_i^2\tilde{H}^{\mathrm{MRC}}_{x_i,l_i}+\hat{H}^{\mathrm{MRC}}_{x_i,l_i}) + \sum_{j\in\mathcal{K}}\sum_{x_j\in\Phi_j/x_i}\frac{P_jG^{\mathrm{MRC}}_{x_j,l_i}}{S_j\|x_j\|^{\alpha}}\Bigg)^{-1}. \quad (23)$$

Using $\int_0^{\infty}e^{-sz}ds = z^{-1}$, the expectation in (23) is evaluated as

$$\mathbb{E}\int_0^{\infty}e^{-t\frac{P_i}{S_ix_i^{\alpha}}(\epsilon_i^2\tilde{H}^{\mathrm{MRC}}_{x_i,l_i}+\hat{H}^{\mathrm{MRC}}_{x_i,l_i})-t\sum_{j\in\mathcal{K}}\sum_{x_j\in\Phi_j/x_i}\frac{P_jG^{\mathrm{MRC}}_{x_j,l_i}}{S_j\|x_j\|^{\alpha}}}dt$$
$$\overset{(a)}{=}\int_0^{\infty}\mathbb{E}e^{-t\frac{P_i}{S_ix_i^{\alpha}}\epsilon_i^2\tilde{H}^{\mathrm{MRC}}_{x_i,l_i}}\mathbb{E}e^{-t\frac{P_i}{S_ix_i^{\alpha}}\hat{H}^{\mathrm{MRC}}_{x_i,l_i}}\mathbb{E}_{\{\Phi_j\}}\mathbb{E}_{\{G^{\mathrm{MRC}}_{x_j,l_i}\}_{x_j,\forall x_j}} \times\prod_{j\in\mathcal{K}}\prod_{x_j\in\Phi_j/x_i}e^{-t\frac{P_j}{S_j}\|x_j\|^{-\alpha}G^{\mathrm{MRC}}_{x_j,l_i}}dt$$
$$\overset{(b)}{=}\int_0^{\infty}\frac{\prod_{j\in\mathcal{K}}\mathbb{E}_{\Phi_j}\prod_{x_j\in\Phi_j/x_i}\mathbb{E}_{G^{\mathrm{MRC}}_{x_j,l_i}}e^{-t\frac{P_j}{S_j}\|x_j\|^{-\alpha}G^{\mathrm{MRC}}_{x_j,l_i}}}{\left(1+t\frac{P_i}{S_ix_i^{\alpha}}\epsilon_i^2\right)\left(1+t\frac{P_i}{S_ix_i^{\alpha}}\right)^{S_i-1}}dt$$
$$= \int_0^{\infty}\frac{e^{-t^{\breve{\alpha}}\tilde{C}(\alpha)\sum_j\lambda_j(\frac{P_j}{S_j})^{\breve{\alpha}}\frac{\Gamma(\breve{\alpha}+S_j)}{\Gamma(S_j)}}}{\left(1+t\frac{P_i}{S_ix_i^{\alpha}}\epsilon_i^2\right)\left(1+t\frac{P_i}{S_ix_i^{\alpha}}\right)^{S_i-1}}dt,$$

where in (a) the independence of *r.v.*s is used, and in (b) we insert the Laplace transforms of *r.v.*s $\tilde{H}^{\mathrm{MRC}}_{x_i,l_i}$, which is a chi-square distributed r.v. with $2(S_i-1)$ DoFs, and $\tilde{H}^{\mathrm{MRC}}_{x_i,l_i}$, which is exponentially distributed, at point $\frac{P_i}{S_i}x_i^{-\alpha}$. In the last step, the following formula is used [50]:

$$\mathbb{E}_{\Phi_j}\prod_{x_j\in\Phi_j}\mathbb{E}_{h_{x_j}}e^{-s_j\|x_j\|^{-\alpha}h_{x_j}} = e^{-\tilde{C}(\alpha)\lambda_js_j^{\breve{\alpha}}\mathbb{E}[h^{\breve{\alpha}}]}, \quad (24)$$

$$I=\int_0^\infty\int_0^\infty \frac{\left(1+(t+\tau)\frac{P_i}{S_i}x_i^{-\alpha}\right)^{-1}\prod_{j\in\mathcal{K}}\mathbb{E}_{\Phi_j}\prod_{x_j\in\Phi_j/x_i}\mathbb{E}_{G^{\mathrm{MRC}}_{x_j,l_i},G^{\mathrm{MRC}}_{x_j,l_i'}}e^{-\frac{P_j(tG^{\mathrm{MRC}}_{x_j,l_i'}+\tau G^{\mathrm{MRC}}_{x_j,l_i'})}{S_j\|x_j\|^\alpha}}}{\left(1+t\frac{P_i}{S_i}\epsilon_i^2x_i^{-\alpha}\right)\left(1+\tau\frac{P_i}{S_i}\epsilon_i^2x_i^{-\alpha}\right)\left((1+t\frac{P_i}{S_i}x_i^{-\alpha})(1+\tau\frac{P_i}{S_i}x_i^{-\alpha})\right)^{S_i-2}}dtd\tau$$
$$=\int_0^\infty\int_0^\infty \frac{\left(1+(t+\tau)\frac{P_i}{S_i}x_i^{-\alpha}\right)^{-1}e^{-\tilde{C}(\alpha)\sum_j\lambda_j(\frac{P_j}{S_j})^{\check{\alpha}}\bar{W}_j(t,\tau)}}{\left(1+t\frac{P_i}{S_i}\epsilon_i^2x_i^{-\alpha}\right)\left(1+\tau\frac{P_i}{S_i}\epsilon_i^2x_i^{-\alpha}\right)\left((1+t\frac{P_i}{S_i}x_i^{-\alpha})(1+\tau\frac{P_i}{S_i}x_i^{-\alpha})\right)^{S_i-2}}dtd\tau, \tag{31}$$

in which $\mathbb{E}(G_j^{\mathrm{MRC}})^{\check{\alpha}}=\frac{\Gamma(\check{\alpha}+S_j)}{\Gamma(S_j)}$ is substituted with G_j^{MRC} which is also a chi-squared r.v. with $2S_j$ DoFs. Finally, substituting Λ defined in Proposition 1 yields

$$\overline{\mathrm{SIR}}^{\mathrm{MRC}}_{x_i,l_i}=\frac{P_iN^r(1-\epsilon_i^2)}{S_ix_i^\alpha}\times\int_0^\infty\frac{e^{-t^{\check{\alpha}}\Lambda}}{\left(1+t\frac{P_i}{S_ix_i^\alpha}\epsilon_i^2\right)\left(1+t\frac{P_i}{S_ix_i^\alpha}\right)^{S_i-1}}dt. \tag{25}$$

To evaluate $\mathrm{Var}(\mathrm{SIR}^{\mathrm{svd}}_{x_i,l_i})$, we need to evaluate $\mathbb{E}\left[\left(\mathrm{SIR}^{\mathrm{svd}}_{x_i,l_i}\right)^2\right]$:

$$\mathbb{E}\left[\left(\mathrm{SIR}^{\mathrm{MRC}}_{x_i,l_i}\right)^2\right]=\frac{(1-\epsilon_i^2)^2N^r(N^r+1)}{P_i^{-2}S_i^2x_i^{2\alpha}}\times\int_0^\infty\int_0^\infty\frac{e^{-(t+\tau)^{\check{\alpha}}\Lambda}}{\left(1+(t+\tau)\frac{P_i}{S_ix_i^\alpha}\epsilon_i^2\right)\left(1+(t+\tau)\frac{P_i}{S_ix_i^\alpha}\right)^{S_i-1}}dtd\tau. \tag{26}$$

Combining (25) and (26), $\mathrm{Var}(\mathrm{SIR}^{\mathrm{svd}}_{x_i,l_i})$ is then obtained as

$$\mathrm{Var}(\mathrm{SIR}^{\mathrm{svd}}_{x_i,l_i})=\frac{(1-\epsilon_i^2)^2N^r}{P_i^{-2}S_i^2x_i^{2\alpha}}\Bigg[(N^r+1)\times\int_0^\infty\int_0^\infty\frac{e^{-(t+\tau)^{\check{\alpha}}\Lambda}}{\left(1+(t+\tau)\frac{P_i}{S_ix_i^\alpha}\epsilon_i^2\right)\left(1+(t+\tau)\frac{P_i}{S_ix_i^\alpha}\right)^{S_i-1}}dtd\tau - N^r\left(\int_0^\infty\frac{e^{-t^{\check{\alpha}}\Lambda}}{\left(1+t\frac{P_i}{S_ix_i^\alpha}\epsilon_i^2\right)\left(1+t\frac{P_i}{S_ix_i^\alpha}\right)^{S_i-1}}dt\right)^2\Bigg]. \tag{27}$$

On the other hand,

$$\mathbb{E}\left[\mathrm{SIR}^{\mathrm{MRC}}_{x_i,l_i}\mathrm{SIR}^{\mathrm{MRC}}_{x_i,l_i'}\right]=\frac{(P_i(1-\epsilon_i^2)N^r)^2}{S_i^2x_i^{2\alpha}}I, \tag{28}$$

where

$$I=\mathbb{E}\left(\frac{P_i}{S_ix_i^\alpha}(\epsilon_i^2\tilde{H}^{\mathrm{MRC}}_{x_i,l_i}+\hat{H}^{\mathrm{MRC}}_{x_i,l_i})+\sum_{j\in\mathcal{K}}\sum_{x_j\in\Phi_j/x_i}\frac{P_jG^{\mathrm{MRC}}_{x_j,l_i}}{S_j\|x_j\|^\alpha}\right)^{-1}\left(\frac{P_i}{S_ix_i^\alpha}(\epsilon_i^2\tilde{H}^{\mathrm{MRC}}_{x_i,l_i'}+\hat{H}^{\mathrm{MRC}}_{x_i,l_i'})+\sum_{j\in\mathcal{K}}\sum_{x_j\in\Phi_j/x_i}\frac{P_jG^{\mathrm{MRC}}_{x_j,l_i'}}{S_j\|x_j\|^\alpha}\right)^{-1}$$
$$=\int_0^\infty\int_0^\infty\frac{\mathbb{E}e^{-\sum_{j\in\mathcal{K}}\sum_{x_j\in\Phi_j/x_i}\frac{P_j}{S_j\|x_j\|^\alpha}(tG^{\mathrm{MRC}}_{x_j,l_i'}+\tau G^{\mathrm{MRC}}_{x_j,l_i'})}}{\left(1+t\frac{P_i}{S_i}\epsilon_i^2x_i^{-\alpha}\right)\left(1+\tau\frac{P_i}{S_i}\epsilon_i^2x_i^{-\alpha}\right)}\times\mathbb{E}e^{-\frac{P_i}{S_ix_i^\alpha}(t\hat{H}^{\mathrm{MRC}}_{x_i,l_i}+\tau\hat{H}^{\mathrm{MRC}}_{x_i,l_i'})}dtd\tau. \tag{29}$$

It is also straightforward to show that

$$\mathbb{E}e^{-\frac{P_i}{S_ix_i^\alpha}(t\hat{H}^{\mathrm{MRC}}_{x_i,l_i}+\tau\hat{H}^{\mathrm{MRC}}_{x_i,l_i'})}=\mathbb{E}e^{-\frac{P_i}{S_ix_i^\alpha}\left(t\sum_{l'\neq l_i}\frac{\|\tilde{\boldsymbol{h}}^\dagger_{x_i,l_i}\boldsymbol{h}_{x_i,l'}\|^2}{\|\tilde{\boldsymbol{h}}_{x_i,l_i}\|^2}+\tau\sum_{l''\neq l_i'}\frac{\|\tilde{\boldsymbol{h}}^\dagger_{x_i,l_i'}\boldsymbol{h}_{x_i,l''}\|^2}{\|\tilde{\boldsymbol{h}}_{x_i,l_i'}\|^2}\right)}$$
$$=\mathbb{E}\exp\Big(-\frac{P_i}{S_ix_i^\alpha}\Big(t\sum_{l'\neq l_i,l_i'}\frac{\|\tilde{\boldsymbol{h}}^\dagger_{x_i,l_i}\boldsymbol{h}_{x_i,l'}\|^2}{\|\tilde{\boldsymbol{h}}_{x_i,l_i}\|^2}+(t+\tau)\frac{\|\tilde{\boldsymbol{h}}^\dagger_{x_i,l_i}\boldsymbol{h}_{x_i,l_i'}\|^2}{\|\tilde{\boldsymbol{h}}_{x_i,l_i}\|^2}+\tau\sum_{l''\neq l_i',l_i}\frac{\|\tilde{\boldsymbol{h}}^\dagger_{x_i,l_i'}\boldsymbol{h}_{x_i,l''}\|^2}{\|\tilde{\boldsymbol{h}}_{x_i,l_i'}\|^2}\Big)\Big)$$
$$=\mathbb{E}e^{-\frac{P_i}{S_ix_i^\alpha}\left(t\sum_{l'\neq l_i,l_i'}\frac{\|\tilde{\boldsymbol{h}}^\dagger_{x_i,l_i}\boldsymbol{h}_{x_i,l'}\|^2}{\|\tilde{\boldsymbol{h}}_{x_i,l_i}\|^2}+\tau\sum_{l''\neq l_i',l_i}\frac{\|\tilde{\boldsymbol{h}}^\dagger_{x_i,l_i'}\boldsymbol{h}_{x_i,l''}\|^2}{\|\tilde{\boldsymbol{h}}_{x_i,l_i'}\|^2}\right)}\times\mathbb{E}e^{-(t+\tau)\frac{\|\tilde{\boldsymbol{h}}^\dagger_{x_i,l_i}\boldsymbol{h}_{x_i,l_i'}\|^2}{\|\tilde{\boldsymbol{h}}_{x_i,l_i}\|^2}}$$
$$=\frac{1}{\left((1+t\frac{P_i}{S_i}x_i^{-\alpha})(1+\tau\frac{P_i}{S_i}x_i^{-\alpha})\right)^{S_i-2}}\frac{1}{1+(t+\tau)\frac{P_i}{S_i}x_i^{-\alpha}}. \tag{30}$$

Inserting (30) in (29), yields Eq. (31), shown on top of this page, where in the last step we apply (24) in which $\bar{W}_j(t,\tau)$ is $\bar{W}_j(t,\tau)=\mathbb{E}\left[(tG^{\mathrm{MRC}}_{x_j,l_i'}+\tau G^{\mathrm{MRC}}_{x_j,l_i'})^{\check{\alpha}}\right]$.

This is then simplified to (9) noting the independence of $G^{\mathrm{MRC}}_{x_j,l_i'}$, and $G^{\mathrm{MRC}}_{x_j,l_i'}$. The proof is completed by obtaining (10) through combining (28) and (31), and inserting the result as well as the obtained formulas for $\mathrm{Var}(\mathrm{SIR}^{\mathrm{svd}}_{x_i,l_i})$ and $\overline{\mathrm{SIR}}^{\mathrm{MRC}}_{x_i,l_i}$ into the definition of SIR correlation coefficient in (8).

REFERENCES

[1] M. G. Khoshkholgh, K. Navaie, K. G. Shin, and V. C. M. Leung, "Coverage performance of MIMO-MRC in heterogeneous networks: A stochastic geometry perspective," in *Proc. IEEE 84th Veh. Technol. Conf. (VTC-Fall)*, Sep. 2016, pp. 1–5.

[2] J. G. Andrews *et al.*, "What will 5G be?" *IEEE J. Sel. Areas Commun.*, vol. 32, no. 6, pp. 1065–1082, Jun. 2014.

[3] F. Boccardi, R. W. Heath, Jr., A. Lozano, T. L. Marzetta, and P. Popovski, "Five disruptive technology directions for 5G," *IEEE Commun. Mag.*, vol. 54, no. 2, pp. 74–80, Feb. 2014.

[4] D. Tse and P. Viswanath, *Fundamentals of Wireless Communication*. Cambridge, U.K.: Cambridge Univ. Press, Sep. 2004.

[5] A. Lozano, R. W. Heath, Jr., and J. G. Andrews, "Fundamental limits of cooperation," *IEEE Trans. Inf. Theory*, vol. 59, no. 9, pp. 5213–5226, Sep. 2013.

[6] H. S. Dhillon, R. K. Ganti, F. Baccelli, and J. G. Andrews, "Modeling and analysis of K-tier downlink heterogeneous cellular networks," *IEEE J. Sel. Areas Commun.*, vol. 30, no. 3, pp. 550–560, Apr. 2012.

[7] H.-S. Jo, Y. J. Sang, P. Xia, and J. G. Andrews, "Heterogeneous cellular networks with flexible cell association: A comprehensive downlink SINR analysis," *IEEE Trans. Wireless Commun.*, vol. 11, no. 10, pp. 3484–3495, Oct. 2012.

[8] A. Guo and M. Haenggi, "Spatial stochastic models and metrics for the structure of base stations in cellular networks," *IEEE Trans. Wireless Commun.*, vol. 12, no. 11, pp. 5800–5812, Nov. 2013.

[9] J. G. Andrews, F. Baccelli, and R. K. Ganti, "A tractable approach to coverage and rate in cellular networks," *IEEE Trans. Commun.*, vol. 59, no. 11, pp. 3122–3134, Nov. 2011.

[10] M. Di Renzo, W. Lu, and P. Guan, "The intensity matching approach: A tractable stochastic geometry approximation to system-level analysis of cellular networks," *IEEE Trans. Wireless Commun.*, vol. 15, no. 9, pp. 5963–5983, Sep. 2016.

[11] M. Di Renzo and P. Guan, "Stochastic geometry modeling of coverage and rate of cellular networks using the Gil-Pelaez inversion theorem," *IEEE Commun. Lett.*, vol. 18, no. 9, pp. 1575–1578, Sep. 2014.

[12] R. Vaze and R. W. Heath, Jr., "Transmission capacity of ad-hoc networks with multiple antennas using transmit stream adaptation and interference cancellation," *IEEE Trans. Inf. Theory*, vol. 58, no. 2, pp. 780–792, Feb. 2012.

[13] A. M. Hunter and J. G. Andrews, "Adaptive rate control over multiple spatial channels in ad hoc networks," in *Proc. 6th Int. Symp. IEEE WiOPT*, Apr. 2008, pp. 469–474.

[14] K. Huang, J. G. Andrews, D. Guo, R. W. Heath, Jr., and R. A. Berry, "Spatial interference cancellation for multiantenna mobile ad hoc networks," *IEEE Trans. Inf. Theory*, vol. 58, no. 3, pp. 1660–1676, Mar. 2012.

[15] R. H. Y. Louie, M. R. McKay, and I. B. Collings, "Open-loop spatial multiplexing and diversity communications in ad hoc networks," *IEEE Trans. Inf. Theory*, vol. 57, no. 1, pp. 317–344, Jan. 2011.

[16] R. Tanbourgi, H. S. Dhillon, and F. K. Jondral, "Analysis of joint transmit–receive diversity in downlink MIMO heterogeneous cellular networks," *IEEE Trans. Wireless Commun.*, vol. 14, no. 12, pp. 6695–6709, Dec. 2015.

[17] M. Di Renzo and P. Guan, "Stochastic geometry modeling and system-level analysis of uplink heterogeneous cellular networks with multi-antenna base stations," *IEEE Trans. Commun.*, vol. 64, no. 6, pp. 2453–2476, Jun. 2016.

[18] M. Di Renzo and P. Guan, "A mathematical framework to the computation of the error probability of downlink MIMO cellular networks by using stochastic geometry," *IEEE Trans. Commun.*, vol. 62, no. 8, pp. 2860–2879, Aug. 2014.

[19] M. Di Renzo and W. Lu, "Stochastic geometry modeling and performance evaluation of MIMO cellular networks using the equivalent-in-distribution (EiD)-based approach," *IEEE Trans. Commun.*, vol. 63, no. 3, pp. 977–996, Mar. 2015.

[20] L. H. Afify, H. ElSawy, T. Y. Al-Naffouri, and M.-S. Alouini, "A unified stochastic geometry model for MIMO cellular networks with retransmissions," *IEEE Trans. Wireless Commun.*, vol. 15, no. 12, pp. 8595–8609, Dec. 2016.

[21] A. K. Gupta, H. S. Dhillon, S. Vishwanath, and J. G. Andrews, "Downlink multi-antenna heterogeneous cellular network with load balancing," *IEEE Trans. Commun.*, vol. 62, no. 11, pp. 4052–4067, Nov. 2014.

[22] T.-X. Zheng, H.-M. Wang, and M. H. Lee, "Multi-antenna transmission in downlink heterogeneous cellular networks under a threshold-based mobile association policy," *IEEE Trans. Commun.*, vol. 65, no. 1, pp. 244–256, Jan. 2017.

[23] Y. Wu, Y. Cui, and B. Clerckx, "Analysis and optimization of inter-tier interference coordination in downlink multi-antenna HetNets with offloading," *IEEE Trans. Wireless Commun.*, vol. 14, no. 12, pp. 6550–6564, Dec. 2015.

[24] S. Mukherjee, "Distribution of downlink SINR in heterogeneous cellular networks," *IEEE J. Sel. Areas Commun.*, vol. 30, no. 3, pp. 575–585, Apr. 2012.

[25] P. Madhusudhanan, J. G. Restrepo, Y. Liu, and T. X. Brown, "Analysis of downlink connectivity models in a heterogeneous cellular network via stochastic geometry," *IEEE Trans. Wireless Commun.*, vol. 15, no. 6, pp. 3895–3907, Jun. 2016.

[26] H. S. Dhillon, M. Kountouris, and J. G. Andrews, "Downlink MIMO HetNets: Modeling, ordering results and performance analysis," *IEEE Trans. Wireless Commun.*, vol. 12, no. 10, pp. 5208–5222, Oct. 2013.

[27] M. G. Khoshkholgh, K. Navaie, K. G. Shin, and V. C. M. Leung, "Performance evaluation of MISO-SDMA in heterogeneous networks with practical cell association," in *Proc. IEEE 84th Veh. Technol. Conf. (VTC-Fall)*, Sep. 2016, pp. 1–5.

[28] Y. Wu, R. H. Y. Louie, M. R. McKay, and I. B. Collings, "Generalized framework for the analysis of linear MIMO transmission schemes in decentralized wireless ad hoc networks," *IEEE Trans. Wireless Commun.*, vol. 11, no. 8, pp. 2815–2827, Aug. 2012.

[29] C. Li, J. Zhang, S. H. Song, and K. B. Letaief, "Analysis of area spectral efficiency and link reliability in multiuser MIMO HetNets," in *Proc. IEEE Int. Conf. Commun. (ICC)*, Jun. 2015, pp. 2839–2844.

[30] S. T. Veetil, K. Kuchi, and R. K. Ganti, "Performance of PZF and MMSE receivers in cellular networks with multi-user spatial multiplexing," *IEEE Trans. Wireless Commun.*, vol. 14, no. 9, pp. 4867–4878, Sep. 2015.

[31] Z. Chen, L. Qiu, and X. Liang, "Area spectral efficiency analysis and energy consumption minimization in multiantenna Poisson distributed networks," *IEEE Trans. Wireless Commun.*, vol. 15, no. 7, pp. 4862–4874, Jul. 2016.

[32] H. H. Yang, G. Geraci, and T. Q. S. Quek, "Energy-efficient design of MIMO heterogeneous networks with wireless backhaul," *IEEE Trans. Wireless Commun.*, vol. 15, no. 7, pp. 4914–4927, Jul. 2016.

[33] R. Hernandez-Aquino, S. A. R. Zaidi, D. McLernon, and M. Ghogho, "Energy efficiency analysis of two-tier MIMO diversity schemes in Poisson cellular networks," *IEEE Trans. Commun.*, vol. 63, no. 10, pp. 3898–3911, Oct. 2015.

[34] A. Shojaeifard, K. A. Hamdi, E. Alsusa, D. K. C. So, J. Tang, and K.-K. Wong, "Design, modeling, and performance analysis of multi-antenna heterogeneous cellular networks," *IEEE Trans. Commun.*, vol. 64, no. 7, pp. 3104–3118, Jul. 2016.

[35] M. G. Khoshkholgh and V. Leung, "On the performance of MIMO-SVD multiplexing systems in HetNets: A stochastic geometry perspective," *IEEE Trans. Veh. Technol.*, vol. 66, no. 9, pp. 8163–8178, Sep. 2017.

[36] M. G. Khoshkholgh, K. G. Shin, K. Navaie, and V. C. M. Leung, "Coverage performance in multistream MIMO-ZFBF heterogeneous networks," *IEEE Trans. Veh. Technol.*, vol. 66, no. 8, pp. 6801–6818, Aug. 2017.

[37] M. Haenggi, "Diversity loss due to interference correlation," *IEEE Commun. Lett.*, vol. 16, no. 10, pp. 1600–1603, Oct. 2012.

[38] R. Tanbourgi, H. S. Dhillon, J. G. Andrews, and F. K. Jondral, "Dual-branch MRC receivers in the cellular downlink under spatial interference correlation," in *Proc. 20th Eur. Wireless Conf.*, May 2014, pp. 13–18.

[39] V. Chandrasekhar, M. Kountouris, and J. G. Andrews, "Coverage in multi-antenna two-tier networks," *IEEE Trans. Wireless Commun.*, vol. 8, no. 10, pp. 5314–5327, Oct. 2009.

[40] J. F. C. Kingman, *Poisson Processes*. London, U.K.: Oxford Univ. Press, 1993.

[41] M. Haenggi and R. K. Ganti, "Interference in large wireless networks," *Found. Trends Netw.*, vol. 3, no. 2, pp. 127–248, 2009.

[42] K. S. Ahn, "Performance analysis of MIMO-MRC systems with channel estimation error in the presence of cochannel interferences," *IEEE Signal Process. Lett.*, vol. 15, pp. 445–448, 2008.

[43] Y. Chen and C. Tellambura, "Performance analysis of maximum ratio transmission with imperfect channel estimation," *IEEE Commun. Lett.*, vol. 9, no. 4, pp. 322–324, Apr. 2005.

[44] R. W. Heath, Jr., and D. J. Love, "Multimode antenna selection for spatial multiplexing systems with linear receivers," *IEEE Trans. Signal Process.*, vol. 53, no. 8, pp. 3042–3056, Aug. 2005.

[45] C. B. Papadias and G. J. Foschini, "On the capacity of certain space-time coding schemes," *EURASIP J. Appl. Signal Process.*, vol. 5, pp. 447–458, May 2002.

[46] S. Jin, M. R. Mckay, X. Gao, and I. B. Collings, "MIMO multichannel beamforming: SER and outage using new eigenvalue distributions of complex noncentral Wishart matrices," *IEEE Trans. Commun.*, vol. 56, no. 3, pp. 424–434, Mar. 2008.

[47] K. R. Kumar, G. Caire, and A. L. Moustakas, "Asymptotic performance of linear receivers in MIMO fading channels," *IEEE Trans. Inf. Theory*, vol. 55, no. 10, pp. 4398–4418, Oct. 2009.

[48] L. G. Ordonez, D. P. Palomar, and J. R. Fonollosa, "Ordered eigenvalues of a general class of hermitian random matrices with application to the performance analysis of MIMO systems," *IEEE Trans. Signal Process.*, vol. 57, no. 2, pp. 672–689, Feb. 2006.
[49] T. H. Cormen, C. E. Leiserson, R. L. Rivest, and C. Stein, *Introduction to Algorithms*, 3rd ed. Cambridge, MA, USA: MIT Press, 2009.
[50] M. Haenggi, J. G. Andrews, F. Baccelli, O. Dousse, and M. Franceschetti, "Stochastic geometry and random graphs for the analysis and design of wireless networks," *IEEE J. Sel. Areas Commun.*, vol. 27, no. 7, pp. 1029–1046, Sep. 2009.

Mohammad G. Khoshkholgh received the B.Sc. degree in electrical engineering from Isfahan University, Isfahan, Iran, in 2006, and the M.Sc. degree in electrical engineering from the Tarbiat Modares University, Tehran, Iran, in 2008. He was with the Wireless Innovation Laboratory, Tarbiat Modares University, from 2008 to 2012. From 2012 to 2014, he was with Simula Research Laboratory, Fornebu, Norway, where he was involved in developing communication solutions for smart grid systems. He is currently with The University of British Columbia. His research interests are mainly in wireless communications and networks. He holds the Vanier Canada Graduate Scholarship.

Keivan Navaie (S'00–M'04–SM'10) is currently with the School of Computing and Communications, Lancaster University, U.K. His research interests lie in the field of mobile computing, radio resource allocation, cognitive radio networks, and cooperative communications. He is on the Editorial Board of the IEEE COMMUNICATIONS SURVEYS AND TUTORIALS, and the IEEE COMMUNICATIONS LETTERS. He has served on the technical program committees of several IEEE conferences, including GlobeCom, ICC, VTC, and WCNC, and chaired some of their symposia. He has also served as Chair of Wireless Network Track, IEEE VTC-2012 Yokohama, Japan, IEEE 8th International Workshop on Wireless Network Measurements WiNMee 2012, Paderborn, Germany, IEEE, Wireless Networks and Security Track, IEEE VTC2014-Spring, Seoul, South Korea, Mobile and Wireless Networks Track, IEEE WCNC 2014, Istanbul, Turkey. He is an IET Fellow and a Chartered Engineer.

Kang G. Shin is currently the Kevin and Nancy O'Connor Professor of Computer Science with the Department of Electrical Engineering and Computer Science, University of Michigan, Ann Arbor, MI, USA. He was a co-founder of a couple of startups and also licensed some of his technologies to industry. His current research focuses on QoS-sensitive computing and networking and embedded real-time and cyber-physical systems.

He has supervised the completion of 80 Ph.D. students, and authored/coauthored over 900 technical articles, a textbook, and over 30 patents or invention disclosures, and received numerous awards, including the 1987 Outstanding IEEE TRANSACTIONS OF AUTOMATIC CONTROL Paper Award, the 2003 IEEE Communications Society William R. Bennett Prize Paper Award, the best paper award from 2010 and 2000 USENIX Annual Technical Conferences, the Best Paper Award from the best paper award from the 2011 ACM International Conference on Mobile Computing and Networking, and the 2011 IEEE International Conference on Autonomic Computing. He has also received several institutional awards, including the Research Excellence Award in 1989, the Outstanding Achievement Award in 1999, the Distinguished Faculty Achievement Award in 2001, and the Stephen Attwood Award from the University of Michigan (the highest honor bestowed to Michigan Engineering faculty) in 2004, the Distinguished Alumni Award of the College of Engineering, Seoul National University, in 2002, the 2003 IEEE RTC Technical Achievement Award, and the 2006 Ho-Am Prize in Engineering (the highest honor bestowed to Korean-origin engineers).

Victor C. M. Leung (S'75–M'89–SM'97–F'03) received the B.A.Sc. degree (Hons.) in electrical engineering from The University of British Columbia (UBC) in 1977 and the Ph.D. degree in electrical engineering from the graduate school at UBC on a Canadian Natural Sciences and Engineering Research Council Postgraduate Scholarship in 1982. From 1981 to 1987, he was a Senior Member of the Technical Staff and a Satellite System Specialist with MPR Teltech Ltd., Canada. In 1988, he was a Lecturer with the Department of Electronics, The Chinese University of Hong Kong. He returned to UBC as a Faculty Member in 1989, where he currently holds the positions of Professor and TELUS Mobility Research Chair in advanced telecommunications engineering with the Department of Electrical and Computer Engineering. He is also serving as the Overseas Dean of the School of Information and Electronic Engineering, Zhejiang Gongshang University, China. He has co-authored over 1000 journal/conference papers, 37 book chapters, and co-edited 12 book titles. Several of his papers had been selected for best paper awards. His research interests are in the broad areas of wireless networks and mobile systems. He is a fellow of the Royal Society of Canada, the Engineering Institute of Canada, and the Canadian Academy of Engineering. He received the APEBC Gold Medal as the head of the graduating class in the Faculty of Applied Science, UBC. He received the IEEE Vancouver Section Centennial Award and the 2011 UBC Killam Research Prize. He was a recipient of the 2017 Canadian Award for Telecommunications Research. He co-authored papers that received the 2017 IEEE ComSoc Fred W. Ellersick Prize and the 2017 IEEE Systems Journal Best Paper Award. He has served on the Editorial Boards of the IEEE JOURNAL ON SELECTED AREAS IN COMMUNICATIONS—Wireless Communications Series and Series on Green Communications and Networking, the IEEE TRANSACTIONS ON WIRELESS COMMUNICATIONS, the IEEE TRANSACTIONS ON VEHICULAR TECHNOLOGY, the IEEE TRANSACTIONS ON COMPUTERS, and the *Journal of Communications and Networks*. He has guest-edited many journal special issues, and provided leadership to the organizing committees and technical program committees of numerous conferences and workshops. He is currently serving on the Editorial Boards of the IEEE WIRELESS COMMUNICATIONS LETTERS, the IEEE TRANSACTIONS ON GREEN COMMUNICATIONS AND NETWORKING, the IEEE TRANSACTIONS ON CLOUD COMPUTING, the IEEE ACCESS, *Computer Communications*, and several other journals. He was a Distinguished Lecturer of the IEEE Communications Society. He is a registered Professional Engineer in the Province of British Columbia, Canada.